

1 **Ductile and brittle deformation in Singapore: a record of Mesozoic orogeny and**  
2 **amalgamation in Sundaland, and of post-orogenic faulting**

3  
4 A. Graham Leslie<sup>\*1</sup>, Thomas J.H. Dodd<sup>1</sup>, Martin R. Gillespie<sup>1</sup>, Rhian S. Kendall<sup>2</sup>, Thomas P.  
5 Bide<sup>3</sup>, Timothy I. Kearsley<sup>1</sup>, Marcus R. Dobbs<sup>3</sup>, Michael Kim Woon Lee<sup>4</sup>, and Kiefer Chiam<sup>5</sup>

6  
7 <sup>1</sup>British Geological Survey, Lyell Centre, Research Avenue South, Edinburgh, EH14 4AP, United Kingdom.

8 <sup>2</sup>British Geological Survey, Cardiff University, Main Building, Park Place, Cardiff, CF10 3AT, United Kingdom.

9 <sup>3</sup>British Geological Survey, Environmental Science Centre, Keyworth, Nottingham, NG12 5GG, United Kingdom.

10 <sup>4</sup>Neptune Court, 8 Marine Vista #15-33, Singapore 449032.

11 <sup>5</sup>BCA Academy, 200 Braddell Rd, Singapore 579700

12 <sup>\*</sup>(Corresponding author e:mail: [agle@bgs.ac.uk](mailto:agle@bgs.ac.uk))

13  
14 **Keywords:** Singapore, Mesozoic, orogeny, fold and thrust tectonics, faulting.

15  
16 **Abstract:** Singapore bedrock geology is dominated by late Permian to Triassic arc magmatism and  
17 a genetically related, essentially Middle to Upper Triassic, marine to fluvial volcano-sedimentary  
18 inner forearc succession. These Mesozoic strata are deformed into a pattern of NE-translated  
19 ductile–brittle deformation structures during the latest Triassic to earliest Jurassic collision and  
20 amalgamation of the Sibumasu continental block with the southern part of the Sukhothai Arc. The  
21 subduction-related magmatic complex represented in Singapore by the granitic to gabbroic plutons  
22 of the Bukit Timah Centre likely acted as a backstop to thrusting at this time. Collisional tectonics  
23 drove progressive shortening and steepened earlier-formed inclined asymmetrical folds,  
24 culminating in the regional-scale development of a non-coaxial, NE-vergent and NE-facing, fold  
25 and thrust system. In Singapore, the Murai Thrust and Pasir Laba Thrust are identified as major  
26 elements of this system; both are associated with SW-dipping thrust-imbricate duplex slices. Two  
27 distinct early Cretaceous (Berriasian and Barremian) sedimentary successions overstep these  
28 collisional tectonic structures. An array of mostly NE–SW and ENE–WSW trending faults and  
29 fractures acts as important control on bedrock unit distribution across Singapore and are most  
30 likely generated by Cenomanian dextral shear stress. That stress locally reactivated faults initiated  
31 during orogeny, or even earlier. Knowledge of the geotechnical impact of these structural features  
32 is critical to both future development and ongoing management of the subsurface in Singapore.

33 [225 words]

34  
35 [10996 words including titles, abstract, captions and references]

37 **1. Introduction**

38 Southeast Asia is made up of a collage of continental blocks and volcanic arc terranes welded  
39 together along suture zones marking the sites of destroyed Tethyan ocean basins (see review in  
40 Metcalfe, 2017). Peninsular Malaysia and Singapore can be geologically described in terms of  
41 three approximately N–S trending tectono-stratigraphical elements, namely the Western, Central  
42 and Eastern belts (Fig. 1A, *cf.* Metcalfe, 2013). The Bentong–Raub Suture Zone forms the  
43 collisional boundary between the Western Belt (essentially the Sibumasu continental block, *cf.*  
44 Metcalfe 2013) and the Central and Eastern belts that contain the rocks making up the Sukhothai  
45 Arc (*cf.* Ng *et al.* 2015a; Gillespie *et al.*, this volume). Previously published geology of Singapore  
46 (DSTA, 2009; Figure 1B) shows many broad-scale similarities with neighbouring Johor in the  
47 southern part of Peninsular Malaysia (*cf.* Hutchison and Tan, 2009) but its structural evolution is  
48 not well understood. The geological relationships in neighbouring Indonesia (Riau Islands  
49 Province) are less well-reported but share many characteristics of the geology in Singapore and  
50 Johor (*cf.* Vilpponen, 1988).

51  
52 The ‘Defence Science and Technology Agency’ (DSTA) commented on a wide range of fold-  
53 and fault-related features in south and southwest Singapore including overturned steep bedding  
54 attitudes (DSTA, 2009). Folds are described as “vertical isoclinal to isoclinal over-folds but are  
55 normally open folds”; fold axes could not be traced for distances greater than a kilometre. Large-  
56 scale folds had been observed at a few localities within the then described ‘Jurong Formation’;  
57 some of those unfortunately are now obscured by development (*cf.* Figures 3.2 and 3.3, DSTA,  
58 2009). DSTA (2009) described fresh examples of Triassic ‘Jurong Formation’ strata as foliated  
59 and recrystallized, with preferred alignments of chlorite, sericite and other micas. Shear fabrics  
60 reported in incompetent beds indicate locally developed high strain and low grade metamorphic  
61 textures (*cf.* Fig. 3.4 in DSTA, 2009).

62  
63 Folding of Triassic strata was thought to have started before sedimentation ceased in the early  
64 Jurassic, and to have been constrained in some manner by the adjacent “buttress of granite”  
65 (DSTA, 2009). At least one example of a north-easterly verging thrust structure interpreted as  
66 “slumping-related” had been reported during construction on the Nanyang Technological  
67 University (NTU) campus. Conversely, the ‘Murai Fault’ was described as having been  
68 “responsible for the dynamic metamorphism of the Triassic sediment” (DSTA, 2009). The  
69 majority of faults affecting Triassic and younger strata, and the plutonic rocks, were understood to  
70 be active in the late Cretaceous (Redding and Christensen, 1999; DSTA, 2009), and again in the  
71 Cenozoic; such tectonic activity was apparently minimal after the Neogene (DSTA, 2009).

72

73 Triassic Semantan Formation rocks in the Central Belt of Peninsular Malaysia show a similar  
74 deformational style to these broadly contemporaneous strata in Singapore, with upright, close to  
75 tight folds and a strong axial planar cleavage (Harbury *et al.*, 1990). Deformation there is attributed  
76 to Upper Triassic dextral transpression, likely associated with collision of Sibumasu and the  
77 Sukhothai Arc (Mustaffa, 2009).

78  
79 From literature and outcrop, the British Geological Survey (BGS) assessed the structural  
80 geology of Singapore for the Building and Construction Authority of Singapore (BCA) in 2014,  
81 confirming that: (i) Triassic strata had been penetratively deformed, folded, and weakly  
82 metamorphosed; and (ii) discrete low-angle south-west dipping and north-east verging thrust  
83 structures (*cf.* Redding and Christensen, 1999) were likely to be responsible for stratigraphical  
84 repetition of Triassic strata. Samples associated with the ‘Murai Fault’ were seen to preserve  
85 variable and locally very intense strain (*cf.* Redding and Christensen, 1999; DSTA, 2009).  
86 Occurrences of phyllonitic rocks previously assigned to the ‘Murai Schist’ (DSTA, 2009)  
87 preserved a penetrative, anastomosing and mylonitic fabric defined by white and pale green micas.  
88 The intensity of strain recorded in those rocks was arguably capable of accommodating several  
89 hundreds of metres displacement, perhaps even a few kilometres (Krabbendam and Leslie, 2010;  
90 Leslie *et al.*, 2010).

91  
92 BGS observed that Triassic strata, and the plutonic igneous rocks of the ‘Singapore’ or Bukit  
93 Timah Granite, had been transected by an array of mostly NNE–SSW trending brittle faults that  
94 had relatively straight traces and were thus likely to be steeply dipping. No definitive fault map  
95 based on observed cut-offs and/or offsets of mapped lithological boundaries existed at that time,  
96 precluding precise summary of the kinematics of these brittle fault arrays. Significant movement  
97 on the faults in Singapore was understood to have largely ceased by the Neogene, (DSTA, 2009).

98  
99 BGS has now analysed data from *c.* 20,000 m of borehole core recovered from 121 *c.* 205 m  
100 deep boreholes commissioned by the BCA (Fig. 2). In addition, we have incorporated new  
101 interpretations of some 218 outcrop locations, predominantly located in southern and southwest  
102 Singapore and its ‘Southern Islands’ (Fig. 1B & Fig.2). In this paper, we report a fully revised  
103 understanding of the ductile and brittle structural geological evolution of Singapore.  
104 Lithostratigraphical units referred to henceforth in this paper cite the fully revised, International  
105 Commission on Stratigraphy (ICS)-compliant, stratigraphical framework and depositional  
106 environment analysis reported fully in Dodd *et al.*, (this volume). That new stratigraphy replaces  
107 the now obsolete ‘Jurong Formation’ of south-west Singapore (Fig. 3). All locations are reported  
108 as geodetic datum SVY21 Singapore co-ordinates.

109 Critical surface exposures in Singapore are somewhat limited; the ‘Southern Islands’ cluster  
110 to the south of mainland Singapore is an important exception (Fig. 1B). The Kent Ridge and  
111 Labrador Park areas in adjacent mainland Singapore are also instructive (K and L on Fig. 1B). In  
112 the west of mainland Singapore, exposures in the Western Water Catchment Live-Firing area  
113 reveal the scale and intensity of thrust-related deformation, including the Murai Thrust structure  
114 described in detail below (M on Fig. 1B).

115

## 116 **2. Regional setting and revised geology of Singapore**

117 Singapore lies at the southern end of the Central Belt and Eastern Belt, 50 to 100 km east of  
118 the projected southerly continuation of the Bentong–Raub Suture Zone (Fig. 1). After the  
119 Sibumasu block rifted from Gondwana during the Permian, its then northward movement was  
120 accommodated by subduction of Palaeo-Tethys ocean crust beneath the Indochina–East Malaya  
121 block from the Permian at least and continuing throughout much of the Triassic. Subduction  
122 processes generated the Sukhothai Arc (Hall, 2009, 2012; Metcalfe, 2011, 2013, 2017 and  
123 references therein). The Permian and Triassic plutonic rocks of Singapore (and the adjacent Riau  
124 Islands) represent the southernmost exposures of the Sukhothai Arc.

125

126 Widely distributed I-type granitoids show Permian and Triassic U/Pb zircon emplacement ages  
127 that reflect the span of arc and back arc development in Peninsular Malaysia and Singapore (c. 265  
128 – 220 Ma, see Oliver *et al.*, 2014; Ng *et al.*, 2015a, b; Searle *et al.*, 2012; Gillespie *et al.*, this  
129 volume). Marine to terrestrial, Devonian to Permo-Triassic, volcano-sedimentary successions in  
130 the Semantan Basin of Peninsular Malaysia are understood to have been deposited as part of this  
131 arc system (Abdullah, 2009).

132

133 The Jurong Group succession records **Middle Triassic** (Anisian to Ladinian) development of  
134 the active forearc in Singapore, and its subsequent brittle–ductile deformation (Figs. 3 & 4, *cf.* Fig.  
135 2, Dodd *et al.*, this volume). Numerous dated units of tuff constrain the age of these strata (c. 242  
136  $\pm 3$  Ma, see Gillespie *et al.* this volume, Winn *et al.*, 2018). Succeeding fluvial to marine Sentosa  
137 Group strata typically lack volcanogenic deposits and may reflect uplift and erosion of the mature  
138 arc. That change is consistent with the relative abundance of conglomerate in the upper part of the  
139 Semantan Basin sequence described by Metcalfe (1990) and may even relate to geodynamic  
140 recovery following slab-break off beneath the Sukhothai Arc (*cf.* Metcalfe, 2017). In Singapore,  
141 two distinct early Cretaceous (Berriasian and Barremian) sedimentary successions overstep the  
142 earlier deformed strata (Fig. 3).

143

144 Figure 4 is a revised bedrock geological map of Singapore based upon our interpretation of all  
145 available new data; the major fold, thrust, and fault structures are superimposed on the principal  
146 lithostratigraphical and lithodemic units; the Jurong and Sentosa groups are shown undivided here  
147 for clarity (*cf.* Figs. 3 & 5). The Murai and Pasir Laba thrusts extend across southwest Singapore,  
148 the former from its ‘type locality’ at Murai Reservoir (Fig. 4). The principal steep, brittle faults  
149 identified onshore and here extrapolated offshore are: the Henderson Road Fault; the Pepys Road  
150 Fault; the Nee Soon Fault; the Seletar Fault and the Bukit Timah Fault Zone (Fig. 4).

### 151 152 **3. Macro- to micro- ductile deformation in the metasedimentary strata of SW Singapore**

153 The Jurong and Sentosa group strata in south-west Singapore record ductile and brittle–ductile  
154 deformation (D1) that can be observed at a variety of scales (see Figs. 4 & 5; Figs. 6, 7 & 8).  
155 Individual, outcrop-scale folds are often apparently upright, open or close but occur within a wider  
156 array of decametre-scale, inclined asymmetrical and close NW–SE striking F1 folds (inset  
157 stereonet, Fig. 5). Microstructural details demonstrate pervasive and penetrative, NE-vergent non-  
158 coaxial deformation (Figs. 7 & 8). Progressive shortening tightened folds during a finite timespan  
159 – in essence a single D1 event. As a consequence, structures became increasingly transposed by  
160 NE-directed tectonic transport. Tightening was achieved through steepening of originally NE-  
161 dipping fold limbs towards, and locally through, the vertical. Significant panels of Jurong and  
162 Sentosa group strata are overturned and inverted by folding; for example, borehole BH2A13  
163 [33778.6 09748.8, Tuas, Fig. 2] has been drilled to a depth of 205.0 m and is all in tightly-folded  
164 inverted strata. The type section for the Tanjong Rimau Formation/Fort Siloso Formation  
165 boundary on Sentosa Island occurs within sub-vertical strata (Dodd *et al.*, this volume). No strictly  
166 isoclinal folds have been observed. The D1 deformation is described further below.

#### 167 168 *D1 deformation, F1 folds and the S1 foliation*

169 The most informative and representative examples of folded Jurong and Sentosa group strata  
170 occur on Pulau Jong (Jong or ‘Junk’ Island), Big Sister’s Island (Pulau Subar Laut) and St John’s  
171 and Lazarus islands (Fig. 6). Elsewhere, systematic variations in dip and/or bedding/cleavage  
172 geometries demonstrate folding (e.g. along South Buona Vista Road in the Kent Ridge area, and  
173 in the Hillside Park, Bukit Batok district (H), see Fig. 1B for locations).

174  
175 On Pulau Jong [22769.9 22039.0, Figs. 2 & 5], Tanjong Rimau Formation sandstone and  
176 conglomerate units are steeply to very steeply dipping. Way-up overall is to the east-northeast  
177 though interrupted by upright metre-scale folding (Fig. 6a). An S1 phyllosilicate schistosity is  
178 well-developed in mudstone interlayers and opposed bedding/cleavage relationships are very clear  
179 on either limb of the exposed folds. On St. John’s Island [29827.8 22611.9, Figs. 2 & 5], Fort

180 Siloso Formation strata show steeply NE-dipping, lenticular cross-bedded fine-grained sandstone  
181 units 1 to 2 cm thick, interbedded with mm-scale layers of planar laminated mudstone; bedding is  
182 right-way-up and younging to the north-east. A clearly-developed, moderately SW-dipping, north-  
183 east facing S1 cleavage is almost perpendicular to bedding and defined by preferred parallel  
184 arrangement of phyllosilicate minerals and a preferred shape fabric in quartz (Fig. 6b).  
185 Bedding/cleavage relationships here demonstrate broadly neutral fold vergence, placing these  
186 outcrops within a local hinge.

187  
188 Right-way up, NE-younging, Fort Siloso Formation heterolithic interbedded sandstone and  
189 siltstone units on Lazarus Island [30169.0 22806.0, Figs. 2 & 5] preserve a sharply refracted S1  
190 cleavage transecting bed boundaries (Fig. 6c). S1 is convergent in mudstone layers and  
191 approximately perpendicular to S0 in sandstone layers (diverging), indicating overall neutral  
192 vergence in a local but large-scale (possibly decimetre to decametre) inclined fold hinge zone.

193  
194 Sandstone-dominated, folded Tanjong Rimau Formation units at Tanjong Lokos on St. John's  
195 Island [30076.6 21788.5, Figs. 2 & 5] demonstrate the progressive nature of the deformation  
196 affecting Jurong and Sentosa group strata. Here, the exposed part of the Lokos Anticline (*cf.* Figure  
197 3.3, DSTA, 2009) is an upright, asymmetrical antiform. Opposed bedding/cleavage relationships  
198 are clear on the adjacent fold limbs, and intense crushing/shearing deformation developed in  
199 sandstone layers located in the inner arc of this structure as the fold tightened (Figs. 6d, 6e & 6f).  
200 The north-eastern limb is much more penetratively deformed than the southwest one, such that an  
201 intense south-west-dipping fracture cleavage is developed even in m-scale thick sandstone layers  
202 (Fig. 6f), strongly implying that the fold became increasingly inclined and overturned towards the  
203 north-east, rotating and shearing the steepening north-eastern limb (Fig. 6d).

204  
205 Discrete folding is rarely observed at core scale. Amongst the best examples are the repeated,  
206 decimetre-scale tight, asymmetrical fold closures that occur in Pulau Ayer Chawan Formation  
207 strata in BH2A12, [31439.2 08515.2, Tuas, Fig. 2], for example the closure at 35.7 m featured in  
208 Fig. 7A. The hinge area of the featured fold demonstrates very clearly the non-coaxial,  
209 anastomosing nature of the S1 foliation in these strata (Fig. 7B). A well-developed grain shape  
210 fabric is observed in the sandstone layer; the boundary between the sandstone and mudstone layers  
211 is transected and offset by micro-shearing characteristic of non-coaxial translational deformation,  
212 rather than flexural folding indicative of simple coaxial shortening. BH2A12 demonstrates clearly  
213 that the most strongly folded intervals of Jurong Group strata are inverted at the broader scale, and  
214 that folding is most intensely developed on the short, overturned limbs of north-east-vergent  
215 asymmetrical folds.

216 At the broader (decametre)-scale in Singapore, outcropping anticlinal fold hinges and closures  
217 dominate such that any complimentary synclinal hinges and closures are apparently lacking in  
218 field and borehole observations. As strain intensifies in these steepening/overturning fold trains,  
219 we would predict a progressive development of penetrative fabrics that intensify downwards onto  
220 discrete thrust discontinuities disrupting the common limbs of asymmetrical fold structures and  
221 underlying synclinal structures. The much larger-scale Murai and Pasir Laba thrusts (see below)  
222 demonstrate this deformational style across southwest Singapore.

223  
224 Across southwest Singapore, the S1 cleavage typically dips south-westwards often displaying  
225 convergent or divergent fans in fold hinges, as constrained by the rheology of the folded strata (*cf.*  
226 Fig. 6). The S1 fabric is readily developed in incompetent Jurong and Sentosa group lithologies;  
227 fine- to very fine-grained sandstone and mudstone layers commonly preserve a penetrative  
228 anastomosing S1 schistosity defined by the preferred parallel alignment of phyllosilicate minerals  
229 and chlorite (Fig. 8a). Lithic clasts become progressively altered to aggregates of fine-grained,  
230 secondary minerals and are increasingly attenuated in the S1 foliation. In contrast, larger quartz  
231 grains remain robust and are wrapped by the new schistosity. Concentrations of iron oxide along  
232 the foliation seams are a common feature where the lithic clasts show progressive alteration and  
233 modification (Fig. 8b). A spaced fracture cleavage is observed locally in more competent  
234 sandstone units, especially so in very steeply-dipping to overturned strata (*cf.* Fig. 6e).

235  
236 Carbonate rocks are strongly affected by pressure solution processes and are characterised by  
237 phyllosilicate-defined S1 foliation seams that are axial planar to microfolds of tectonically-  
238 generated stylolite seams (Figs. 8c, 8d & 8e). The S1 foliation deflects around macrofossil  
239 fragments leaving the latter largely intact (Fig. 8d). Tuffaceous rocks do not typically become  
240 foliated or cleave penetratively; in thin section sericitic/chloritic alteration products are arranged  
241 as anastomosing linear trails aligned parallel to the penetrative S1 cleavage in more incompetent  
242 lithologies interlayered with the volcanogenic strata (Fig. 8f). The implied grade of metamorphism  
243 is never greater than lowermost epizone (prehnite-pumpellyite facies) with no development of sub-  
244 grain morphologies observed in quartz.

#### 245 246 **4. Progressive deformation in the Murai Thrust Belt**

247 The Western Water Catchment/SAFTI Live Firing area in Western Singapore exposes critical  
248 detail of the Murai Thrust structure (Figs. 1 & 4). At Murai Reservoir, excavations have created  
249 three-dimensional outcrops that reveal the complexity of features in the hanging wall of the Murai  
250 Thrust (Fig. 9). The line interpretation shown in the lower panel of Figure 9 includes the principal  
251 dislocation surfaces; the overall antiformal nature of this particular thrust stack; the discrete faults

252 accommodating extensional surge on the leading edge of the stack; and the over-steepened ramp  
253 that now lies within the sub-vertical imbricate structure of the trailing edge of the overall structure.  
254 The variability in structural attitude revealed here is a clear indication of what should locally be  
255 anticipated elsewhere along the trace of the Murai and Pasir Laba thrusts, superimposed upon any  
256 broader-scale variability in bedding dip that results from folding in those same areas. Shearing  
257 deformation has been observed in outcrop in former excavations off Pepys Road, Bukit Panjang  
258 (Figure 3.4 in DSTA, 2009), coincident with the south-eastern part of the Murai Thrust trace.

259  
260 At Murai Reservoir, an anastomosing, sinuous penetrative fabric is ubiquitous; any discrete  
261 lithological units that can be identified are lenticular at all scales in response to the intense shearing  
262 deformation (Fig. 10). At the larger scale, this lenticular geometry is apparent in the arrangement  
263 of the pale greyish-white quartz-arenite layers that are outlined on Figure 9 in the central part of  
264 the antiformal stack. Secondary shears cut across the earlier-formed shear fabric; that secondary  
265 stacking culminates in formation of the observed antiformal stack (Figs. 9 and 10). Grain-scale  
266 attenuation of original clasts is demonstrated by elongated quartz clasts on foliation surfaces that  
267 also preserve a weak mineral-stretching lineation aligned parallel to the long axes of these clasts  
268 and demonstrating top-to-the NE tectonic transport (050°N).

269  
270 Petrographic examination (Fig. 11), of these intensely deformed rocks indicates that:  
271 a) deformation affects units of sandstone, volcanoclastic sandstone, mudstone and tuff that  
272 can all now be assigned to the Boon Lay Formation (Jurong Group, Dodd *et al.*, this  
273 volume);  
274 b) the grade of metamorphic recrystallisation is always low (lowermost epizone with no  
275 development of sub-grain morphologies in quartz); and  
276 c) the sense of shear is consistently top to the north-east, as constrained by the measured  
277 lineations at outcrop.

278  
279 At the broader scale across south-west Singapore, the Murai Thrust places the older Pulau  
280 Ayer Chawan, Pandan, and lower parts of Boon Lay, formations structurally over the upper  
281 (younger) parts of the Boon Lay Formation, including the distinctive Clementi Member. The Pulau  
282 Ayer Chawan and Pandan formations have not been identified in the near surface in the footwall  
283 of the Murai Thrust, either at outcrop or in the numerous boreholes in this region (Figs. 1B and 2).  
284 Thin remnants of Tanjong Rimau Formation strata are identified locally in the hanging wall of the  
285 Murai Thrust structure in the Kent Ridge area (in BH1F5, Fig. 2, Dodd *et al.* this volume). The  
286 limited occurrences of Tanjong Rimau Formation strata that occur to the north-west of the  
287 Henderson Road Fault contrast sharply with the much greater thicknesses found to the south-east

288 of the same fault (Fig. 4). This disparity argues strongly that significant (down-to-the-SE)  
289 displacement must have occurred on the Henderson Road Fault, prior to any fold and thrust  
290 deformation (see further discussion below).

291  
292 Strongly deformed, locally mylonitic, Buona Vista Formation strata are conspicuous in the  
293 footwall of the Murai Thrust (Fig. 4); unconformably overlying older Boon Lay Formation strata  
294 (Dodd *et al.*, this volume). A similar relationship is preserved in the immediate footwall of the  
295 Pasir Laba Thrust on the NTU campus (NTU on Fig.4). There, feature mapping based on 1976  
296 vintage B&W aerial photography (pre-dating campus development) constrains limits on the  
297 distribution of sheared Buona Vista Formation strata (BH1B1 and BH1B2, Fig. 2) that are clearly  
298 discordant and overstepping with respect to folded Pulau Ayer Chawan, Pandan and Boon Lay  
299 Formation strata (Dodd *et al.*, this volume). A syn-deformation ‘piggy back’ depositional setting  
300 is proposed for these distinctive conglomeratic strata (*cf.* Ori and Friend, 1984).

301  
302 The scale of displacement on the Murai Thrust cannot directly be constrained by measurement  
303 but the style of deformation, and the thickness of phyllonitic rocks exposed at Murai Reservoir,  
304 suggests that NE-directed translation on a scale of several hundred metres, even a few kilometres,  
305 is possible (Figs. 9, 10 and 11).

## 306 307 **5. Deformation model, sub-surface architecture, and the timing of deformation**

308 Shortening locally culminated in the disruption and attenuation of steepening and overturning  
309 limbs as strain became partitioned, leading to the development of a large-scale NE-vergent thrust  
310 system, elements of which are distributed all across south-west Singapore (Fig. 4). The long limbs  
311 of the hanging wall anticline structures above thrusts are more broadly flat-lying though  
312 undulating, displaying open to close upright folding at  $< 1$  km wavelength. In lower strain regions,  
313 bedding dips either to the north-east or, more commonly, to the south-west. Any tectonic foliation  
314 typically dips moderately to steeply south-west. At locations where the orientation of bedding and  
315 the S1 fabric can be directly compared, a small clockwise transection angle is observed (*c.* 5°, S1  
316 on bedding) suggesting that this ductile deformation is, strictly speaking, dextrally transpressive.

317  
318 A composite model for the ductile deformation affecting the Jurong and Sentosa group strata  
319 in south and south-west Singapore is summarised in the schematic cross-section of Figure 12.  
320 Tectonic transport overall is towards the north-east. In relatively low strain areas, such as Tanjong  
321 Lokos on St. John’s Island, folds are asymmetrical but broadly upright. In higher strain volumes,  
322 bedding would be progressively steepened and transposed on the north-eastern limbs of fold sets  
323 such that the stratigraphy becomes increasingly tightly folded, more strongly cleaved, and more

324 typically inverted, e.g. as seen in the boreholes in northern Tuas (*cf.* Fig. 7). Ultimately, gently to  
325 moderately dipping laterally extensive thrust discontinuities are developed, such as the Murai (and  
326 Pasir Laba) Thrust. Strata are intensely deformed in the immediate hanging wall of these  
327 structures, thrust over younger strata such as the Boon Lay Formation in the Hillside Park region  
328 of Bukit Batok (see Fig. 1B for location).

329  
330 The structural evolution and broad-scale architecture of the (meta)sedimentary strata in south-  
331 west Singapore is illustrated in Figure 13. These cross-sections illustrate the geometry of the  
332 folding that affects the Jurong and Sentosa group strata as well as the gross ‘older-over-younger’  
333 nature of the discontinuities associated with the Murai Thrust and the related Pasir Laba Thrust.  
334 Deformation and displacement expressed at such a scale means that it is appropriate to regard the  
335 panel of lithostratigraphy transported in the hanging wall of the Murai Thrust as constituting a  
336 thrust nappe, named here as the Murai Nappe (Fig. 13). As currently understood, the Pasir Laba  
337 Thrust is associated with intraformational offsets of Pulau Ayer Chawan and Pandan formation  
338 strata and possibly represents rather smaller-scale shortening within the Murai Nappe, presumably  
339 preceding major translation and shortening accommodated on the structurally lower Murai Thrust  
340 structure.

341  
342 The position of the Buona Vista Formation strata in the immediate footwall of the Pasir Laba  
343 Thrust is clear (around BH1B1 and BH1B2 on Fig. 13); likewise, the unconformable overstep of  
344 the earlier orogenic deformation that occurs at the base of the Bukit Batok Formation (around  
345 BH2B4). The interpreted multiple strands of the Bukit Timah Fault Zone are shown around the  
346 location of BH2B5 on figure 13; also shown are the likely moderate to steeply-dipping nature of  
347 the intrusive contacts within the Bukit Timah Centre.

348  
349 Fold and thrust deformation in Singapore is clearly superimposed on Jurong and Sentosa group  
350 strata whose age is now well-constrained by U/Pb zircon dating (Dodd *et al.*, this volume; Gillespie  
351 *et al.* this volume; Winn *et al.* 2018). Numerous intervals of tuff interbedded with the Pulau Ayer  
352 Chawan, Pandan and Boon Lay formation strata all were erupted at *c.* 242 Ma. The youngest U/Pb  
353 detrital zircon age recorded to date in Tanjong Rimau Formation strata (209 Ma, Oliver *et al.*,  
354 2014) shows that orogenic collision of Sibumasu and the Indochina–East Malaya block must have  
355 culminated after this date, at least in the future Singapore region. The youngest dated S-type  
356 granites in the Western Belt of Peninsular Malaysia are *c.* 195 – 200 Ma (U/Pb zircon, Liew and  
357 McCulloch, 1985; Ng *et al.*, 2015b) suggesting that collision was essentially complete by this time  
358 in the earliest Jurassic. No more refined age constraints are currently available from Singapore; no  
359 other Jurassic strata are known to occur in Singapore and the next youngest strata overstepping the

360 fold and thrust deformation are believed to be no older than Berriasian in age (<145 Ma, Dodd *et*  
361 *al.*, this volume).

362

## 363 **6. Brittle deformation and the large-scale pattern of faulting in Singapore**

364 The most significant fault features which can be interpreted in the current understanding of the  
365 bedrock geology of Singapore are arrays of NE–SW, NNW–SSE, and NW–SE striking  
366 discontinuities (Fig. 4). Brittle deformation leading to faulting is an important factor in the  
367 geological evolution of Singapore and is a very significant constraint on the distribution of  
368 lithological units in the sub-surface. However, very few faults are actually exposed in the modern  
369 urban landscape of Singapore; modern imagery (satellite or similar) is severely compromised by  
370 that landscape. Positional inferences can be drawn from physiographical features captured in 1976-  
371 vintage B&W aerial photography that pre-dates much of this urban landscape, and from offset  
372 geological features, as well as from an assessment of publically available marine bathymetrical  
373 data. The majority of brittle faults in Singapore bedrock are likely to be very steeply dipping or  
374 sub-vertical, judging by the relatively straight fault traces interpreted from the currently available  
375 data. Those observed in outcrop are small-scale features with centimetre- to decimetre-scale  
376 displacements typically; no natural exposure of cataclasite, or other fault rock is known. Most of  
377 the new BCA-commissioned ground investigation boreholes were drilled vertically, and virtually  
378 none of them have intersected major faults.

379

380 Only a handful of fault features have been named previously (DSTA, 2009; Oliver and Gupta,  
381 2019). These include the Henderson Road, Pepys Road, Nee Soon, and Seletar faults, and the Bukit  
382 Timah Fault Zone. Given the orientation of this fault array (Fig. 4), and the regional-scale  
383 Mesozoic/Cenozoic stress regime (and thus  $\sigma_1$ ), it is likely that many of the individual fault  
384 features in these arrays will have been re-activated, perhaps multiple times, since the end of the  
385 Triassic and throughout the Cenozoic.

386

### 387 *6.1 Bukit Timah Fault Zone*

388 The Bukit Timah Fault Zone (BTFZ on Fig. 4) is the largest and arguably most important  
389 discontinuity in Singapore. The BTFZ essentially delineates the boundary between the plutonic  
390 rocks of the Bukit Timah Centre and the (meta)sedimentary Jurong and Sentosa group strata to the  
391 south-west. Occurrences of Lower Cretaceous Bukit Batok Formation strata are spatially  
392 associated with this structure, apparently occurring as fault-bound lenses arranged within the fault  
393 damage zone. Despite its size, the BTFZ is not currently exposed anywhere at surface, and its  
394 character and even its precise location is not well understood. Borehole BH2F5 [21620.8 34315.0,  
395 Bukit Batok, Fig. 2] is the only available borehole that clearly intersects a major strand of the

396 BTFZ juxtaposing igneous and metasedimentary rock. The distribution and character of  
397 deformation in the cored interval indicates that cataclasite and more intensely ductile-deformed  
398 mylonitic rock was produced more or less contemporaneously, with the cataclasite representing  
399 'failure' zones in the rock mass or in damage zones that otherwise responded to strain in a more  
400 brittle–ductile fashion.

401  
402 There is little evidence to constrain the size of the horizontal displacement on the BTFZ; the  
403 fact that plutonic igneous rocks and sedimentary/metasedimentary rocks are juxtaposed across it  
404 indicates that the vertical displacement is at least several, and possibly as much as ten, kilometres.  
405 A fault of that size will have formed as a set of anastomosing strands within a fault zone that  
406 pinched and swelled vertically and laterally. Thus, in places the structure may consist of a single  
407 substantial strand, while elsewhere several smaller strands may accommodate strain as  
408 demonstrated in the closely spaced BH2B6 and BH1B10 borehole arrays (Fig. 2), (see Fig. 14).

409  
410 The BTFZ is displaced locally by NE–SW striking structures. That, and the range of mylonitic  
411 and cataclastic fault rocks intersected in boreholes, implies that this structure has a long and  
412 complex history. The oldest displacement on the BTFZ for which direct evidence has been  
413 observed has a brittle–ductile style of deformation. However, the size of the vertical displacement  
414 alone (perhaps around 10 kilometres) required to juxtapose the Bukit Timah Centre and  
415 metasedimentary Jurong Group strata, suggests an earlier, possibly essentially ductile, phase of  
416 displacement would have been involved. The oldest intrusion in the Bukit Timah Centre, the Choa  
417 Chu Kang Granodiorite–tonalite Pluton, crops out on the north-east side of the BTFZ, and is the  
418 only part of the Bukit Timah Centre to display a widely developed tectonic fabric (Gillespie *et al.*,  
419 this volume). A band of mylonite around 17 metres thick (true thickness) dipping east at 55°, is  
420 developed within the granodiorite of borehole BH1E4 [20773.3 39668.1, Fig. 2], approximately 3  
421 km from the nearest part of the BTFZ trace; other such deformation zones in this pluton may occur  
422 in unsampled ground. This zone of ductile 'shear' may be typical of structures that accommodated  
423 the earliest displacements on a 'proto-BTFZ'. Such structures may have accommodated much of  
424 the early, reverse displacement that brought parts of this pluton to shallower levels in the middle  
425 part of the Permian Period (i.e. before younger plutons lacking a tectonic fabric were emplaced in  
426 the Bukit Timah Centre, Gillespie *et al.*, this volume). As the rock mass moved to shallower levels,  
427 perhaps accompanied by a contemporaneous reduction in regional compressive stress, the  
428 deformation became more focussed and more brittle, creating much the damage zone encountered  
429 today in the BTFZ.

430

431 Some control upon the patterns of deposition in the Jurong Group strata across the alignment  
432 of any ‘proto-BTFZ’ cannot be ruled out (*cf.* Oliver and Prave, 2013; Oliver and Gupta, 2019). A  
433 ‘proto-BTFZ’ structure may have partially accommodated uplift of the arc plutonic complex so  
434 that erosion then supplied granitic detritus into the Tanjong Rimau Formation depocentre (*cf.* Dodd  
435 *et al.*, this volume). In addition, it seems likely that the plutonic rocks of the Bukit Timah Centre  
436 will have acted as a backstop to thrusting and ductile deformation in the latest Triassic to earliest  
437 Jurassic, so that the fault zone may have accommodated very significant movements at this time.  
438 Later, the structure is suitably orientated to act as a P-shear during late Cretaceous dextral shear  
439 (Fig.4 inset; *cf.* Hutchison and Tan, 2009).

440

#### 441 6.2 Henderson Road Fault

442 The Henderson Road Fault (HRF on Fig. 4) is one of the most prominent fault structures now  
443 identified in Singapore but is not exposed in any section today. As originally identified (DSTA,  
444 2009), the Henderson Road Fault follows the line of the modern roadway of that name but does  
445 not appear as a significant feature on the aerial photography that pre-dates the modern urban  
446 development and the present-day road alignment. It is apparent however that there is a marked  
447 change in distribution of pre-Cretaceous and Cretaceous strata across the fault zone, which is  
448 interpreted to extend from the Fort Canning area, across the Kent Ridge/Mount Faber area (K on  
449 Fig.1B), and apparently continuing south of Jurong Island. The extent to which this fault can be  
450 traced to the north-east of the BTFZ is not clear, but it is likely to have been re-activated locally  
451 at least during any Cretaceous strike-slip faulting.

452

453 The revised trace for the Henderson Road Fault separates older Jurong Group strata (Pulau Ayer  
454 Chawan, Pandan and Boon Lay formations) that dominate the north-western wall of the fault from  
455 the younger Sentosa Group strata (Tanjong Rimau and Fort Siloso formations) that dominate the  
456 south-east wall of the fault (Figs. 4 & 5). This abrupt change in preserved lithostratigraphical level  
457 suggests that significant (down-to-the-SE) displacement occurred across the trace of what is now  
458 the Henderson Road Fault, prior to fold and thrust deformation. Other (E)NE–(W)SW trending  
459 structures may have been similarly active at this time. The Henderson Road Fault apparently bends  
460 from an ENE–WSW to a NE–SW strike in the Kent Ridge to Fort Canning area forming a  
461 (sinistral) pull-apart feature in conjunction with the Pepys Road Fault; the north-western limit of  
462 the pull-apart structure marks the north-western extent of the Kusu Formation (Dodd *et al.*, this  
463 volume; Fig. 4).

464

#### 465 6.3 Pepys Road Fault

466 This fault (PRF on Fig. 4) has not been encountered in the new borehole cores, or at outcrop.  
467 A slightly revised trace does however coincide with a significant NE–SW trending topographical  
468 feature and mappable offsets of geological boundaries between Kent Ridge and Telok Blangah  
469 (Fig. 1B; *cf.* DSTA, 2009). It should be noted that although Kusu Formation strata have been  
470 identified at Telok Blangah (south-east of the Pepys Road Fault), the formation has not been  
471 identified anywhere to the north-west of the PRF. Our geological interpretation suggests that this  
472 fault will have likely been hard-linked to a significant extent with the Henderson Road Fault,  
473 sharing at least part of their displacement history.

474

#### 475 *6.4 Nee Soon Fault and Seletar Fault*

476 The traces of these fault structures (NST and SF on Fig. 4), have not been significantly modified  
477 from previous interpretations (DSTA, 2009), though some minor adjustments have been made  
478 locally to account for topography. There is a strong spatial association between the Nee Soon Fault  
479 and the western limit of the Bedok Formation against the plutonic rocks of the Bukit Timah Centre.  
480 However, the extent to which this fault (or the Seletar Fault) may have been active before, during,  
481 or after deposition of the Bedok Formation remains unclear however (*cf.* Dodd *et al.*, this volume).

482

483 Significant movement on the faults in Singapore appears to have largely ceased by the time the  
484 Bedok Formation was deposited in the Neogene or later. Minor offsets of bedding reflectors  
485 detected in new seismic data acquired by BCA in the Seletar/Punggol area have been interpreted  
486 by BGS as possible fault offsets affecting Bedok Formation strata, but no borehole core that would  
487 allow this to be tested has been recovered from the offset reflector package. A regional  
488 consideration of fault history suggests that Cenozoic movements are likely on suitably oriented  
489 faults (see review in Hutchison and Tan, 2009).

490

## 491 **7. Discussion: Mesozoic to Cenozoic geological evolution of Singapore**

### 492 *7.1 Mesozoic collision*

493 A single progressive D1 ductile to brittle–ductile deformation is recorded throughout the  
494 Jurong and Sentosa group (meta)sedimentary and volcanogenic strata that dominate the sub-  
495 surface geology of south and south-west Singapore, including the offshore islands in that region.  
496 Deformation is very strongly partitioned, the highest strains being expressed on discrete NE–  
497 vergent thrust structures that disrupt the developing NW–SE striking and NE-vergent fold patterns.  
498 The most important of these thrust structures is the Murai Thrust; the related Pasir Laba Thrust  
499 sub-divides the Murai Nappe (Fig. 13). Fold structures are typically inclined and overturned when  
500 viewed at decametre-scale. Fold axes are generally sub-horizontal to gently SE-plunging overall,  
501 though NW-plunges may be anticipated locally. Folding thus has a very significant impact on the

502 geology of south and south-west Singapore and is responsible for the wide range of bedding dip  
503 values, including panels of overturned strata. Thrust structures will create low-angle high-strain  
504 discontinuities in the sub-surface.

505  
506 Jurong and Sentosa group strata record metamorphic conditions that, at maximum, are  
507 equivalent to lowermost epizone (prehnite-pumpellyite facies); new minerals such as sericite mica,  
508 chlorite, and epidote show a preferred parallel alignment growing on penetrative foliation surfaces  
509 that are a consequence of non-coaxial (translational) deformation processes. Quartz overgrowths  
510 on original detrital quartz grains are very well-developed. Growth of new phyllosilicate minerals  
511 and epidote means that Jurong Group strata in particular are pervasively recrystallized to the extent  
512 that no primary porosity survives. Sentosa Group strata, and especially the Tanjong Rimau  
513 Formation strata, are more open-textured locally and may retain a greater degree of primary  
514 depositional porosity, suggesting slightly shallower burial after compaction and deformation than  
515 the Jurong Group strata.

516  
517 Deposition of the Jurong Group strata was broadly contemporaneous with the emplacement  
518 of the various plutons that make up the Bukit Timah Centre. Tuffs and tuffaceous sandstones form  
519 a conspicuous element of the Pandan, Pulau Ayer Chawan, and Boon Lay formations of the Jurong  
520 Group succession, with the maximum development of eruptive volcanic activity at *c.* 242 Ma  
521 (Dodd *et al.*, this volume; Gillespie *et al.*, this volume). The younger Sentosa Group strata contain  
522 abundant eroded volcanic detritus and so apparently post-date the period of active arc magmatism  
523 (*cf.* Dodd *et al.*, this volume). Indeed, given that uplift and erosion was now apparently affecting  
524 the mature Sukhothai Arc, it may be that deposition of the Sentosa Group coincided with the timing  
525 of break-off of the old Paleo-Tethys oceanic slab. In any case, deformation in the Jurong and  
526 Sentosa group strata is thus younger than the period spanned by active arc magmatism (Fig.15, *cf.*  
527 Metcalfe 2017).

528  
529 Polyphase ductile deformation and greenschist facies (biotite grade) metamorphism has  
530 affected Sajahat Formation strata found in the eastern (Pulau Sajahat) and northern (Punggol) parts  
531 of Singapore (Gillespie *et al.*, this volume; Oliver and Gupta, 2019). That polyphase deformation  
532 in Sajahat Formation strata is now understood to be Carboniferous in age (Oliver and Gupta, 2019),  
533 is clearly overprinted by the contact metamorphic effects of the developing Bukit Timah Centre  
534 plutons (DSTA, 2009), and so must wholly predate the age span of the active arc magmatism and  
535 the subsequent deformation of the Jurong and Sentosa group strata. We find no clear evidence of  
536 any pervasive tectonic overprint in Sajahat Formation rocks that might be related to the  
537 deformation events recorded in the younger Jurong and Sentosa group strata.

538 The age of the ductile deformation affecting the Jurong Group and Sentosa Group strata must  
539 post-date the youngest analysed detrital zircon reported from strata that are now assigned to the  
540 Sentosa Group Tanjong Rimau Formation (*c.* 209 Ma; Oliver *et al.*, 2011, 2014; *cf.* Dodd *et al.*  
541 this volume). It is possible, though currently unproven, that deposition of the Sentosa Group could  
542 have extended from the uppermost Triassic into the earliest Jurassic after 201.3 Ma. The  
543 deformation recorded in Singapore suggests strongly that the last stages of closure of Palaeo-  
544 Tethys and the consolidation of Sundaland must also have straddled the Triassic/Jurassic boundary  
545 (*cf.* Carter *et al.*, 2001; Hutchison and Tan, 2009; Metcalfe, 2017; Zhang *et al.*, 2019),  
546

547 We attribute deformation of the Jurong and Sentosa group strata of Singapore to the final  
548 stages of broadly east-directed (present day co-ordinates) suturing and amalgamation of the  
549 southern regions of Sibumasu and the Sukhothai Arc with the Indochina–East Malaya block  
550 (Fig.15). Other authors (e.g. Sone and Metcalfe, 2008, Sevastjanova *et al.*, 2011; Metcalfe, 2013,  
551 2017; Oliver *et al.*, 2014, Ng *et al.*, 2015b) have argued that collision of Sibumasu with the ocean-  
552 facing margin of the Sukhothai Arc across the Bentong–Raub Suture Zone occurred during the  
553 Late Triassic, and followed Early Triassic, Permian, or older deformation events attributed  
554 separately to accretion in the Bentong–Raub Suture Zone or to back-arc collapse and suturing of  
555 the Sukhothai Arc onto Indochina–East Malaya. These events have all been cited as parts of the  
556 Indosinian Orogeny leading to the assembly of ‘proto-Southeast Asia’ and Sundaland (*op.cit.*),  
557 following on from an original designation of ‘Indosinian’ in reference to tectonic events affecting  
558 Vietnam (Fromaget, 1938, 1941; *cf.* Tran van Tri, 2011). It is clear that orogenic deformation  
559 affecting the Jurong and Sentosa group strata in Singapore can only have succeeded deposition  
560 (after 209 Ma at least), and therefore occurred close to the Triassic/Jurassic boundary. This implies  
561 that strain accommodating final amalgamation and consolidation of Sundaland must have  
562 continued, if only locally, until this time. Oliver *et al.* (2014) proposed that Sibumasu overrode the  
563 Indochina–East Malaya Block during terminal stages of collision – the north-east-vergent  
564 accretionary tectonics observed in the Mesozoic strata of Singapore are consistent with this model.  
565 **These more recent observations suggest that further regional-scale investigation would be of value**  
566 **in Johor and other parts of Peninsular Malaysia, and including Singapore and the adjacent Riau**  
567 **Islands.**  
568

## 569 7.2 Patterns of faulting in Singapore, regional stress and the timing of brittle deformation

570 Taken together, the full array of (E)NE–(W)SW, NNW–SSE, and NW–SE (and N–S) striking  
571 fault structures that transect the Singapore region (Fig. 4), fit well with a dextral shear regime in  
572 which the maximum compression direction ( $\sigma_1$ ) is oriented about 010 to 190°N (Fig.4 inset).  
573 NNW–SSE oriented fractures would equate to R1 Riedel shears (dextral); NE–SW oriented

574 fractures to R2 Riedel shears (sinistral, as observed); and the subsidiary N–S fractures would  
575 equate to extension/normal faults in this regime. The NE–SW trending features are very likely to  
576 have formed by re-activation of fractures formed as ductile deformation, folding and thrusting  
577 waned and the stacked and deformed Jurong and Sentosa group strata cooled.

578  
579 NW–SE oriented fractures, such as the BTFZ, would equate to P-shears (dextral) in this late  
580 Cretaceous regional stress regime; and ENE–WSW oriented fractures would equate to X-shears  
581 (sinistral, as observed). These last two fracture sets typically form somewhat later than the R1, R2  
582 Riedel shears as strain intensifies in the same regional stress regime; in this case, ENE–WSW  
583 striking faults aligned with the Singapore Strait seem to be the longest-lived (X) shears in the array  
584 as a whole and perhaps were reactivated later still in the Cenozoic. The R1, R2 Riedel shear offsets  
585 in this array seem typically to be small (of the order of 100 m or less, apparent left-lateral offset  
586 for R2); the X-shears seem to represent larger offsets of perhaps 500 m or so. In the absence of  
587 any tightly constrained fault cut-off data these estimates are however speculative.

588  
589 The orientation of these fracture sets is consistent with an array of fractures associated with a  
590 dextral strike-slip principal displacement zone aligned sub-parallel to Peninsular Malaysia (*cf.* Bok  
591 Bak Fault Zone, Hutchison and Tan, 2009, p263). This deformation would likely have strongly  
592 overprinted any earlier brittle deformation developed towards the end of the waning fold and thrust  
593 deformation.

594  
595 Dating of these long-lived structures is relative and unclear. There is no direct-dating evidence  
596 for the age of any fault structures in Singapore. Faulting clearly disrupts the Permo-Triassic  
597 plutonic igneous rocks of the Bukit Timah Centre. Faulting also clearly offsets the Triassic Jurong  
598 Group, Sentosa Group, and Lower Jurassic Buona Vista Formation lithostratigraphy and the  
599 patterns of ductile deformation that formed prior to, and after, the latest Triassic to earliest Jurassic  
600 brittle-ductile fold and thrust deformation. The Kusu and Bukit Batok formation strata are also  
601 clearly affected so that a significant component of the brittle (strictly fault-related) deformation  
602 must post-date deposition of these Lower Cretaceous strata. Tectonic activity appears to be much  
603 reduced after deposition of the Bedok Formation, though the western boundary of this formation  
604 against the granitic rocks of the Bukit Timah Centre is likely to have been modified to some extent  
605 by faulting (Nee Soon Fault, DSTA, 2009).

606  
607 Hutchison and Tan (2009) concluded that dextral shear affected Peninsular Malaysia in the  
608 late Cretaceous, with subsequent sinistral reactivation of the fault systems in the Cenozoic. A  
609 modern systematic appraisal is lacking; a late Cretaceous to early Cenozoic (Palaeogene, <95 Ma)

610 age for this extensive pattern of faulting across Singapore seems realistic and would allow for  
611 some localised reactivation after deposition of the Bedok Formation in the last two million years  
612 or so.

613

### 614 7.3 Current *in situ* stress regime

615 A number of studies of the current *in situ* stress regime have been undertaken in Singapore  
616 using hydraulic fracturing methods (Zhao *et al.*, 2005; Winn and Ng, 2013; Meng *et al.*, 2012).

617 While there is some variability in the results, there is also broad agreement on the following:

- 618 • the setting is a thrusting regime ( $\sigma_H > \sigma_h > \sigma_v$ )
- 619 • maximum horizontal stress is oriented NNE–SSW
- 620 • maximum principal stress varies from approximately 3 – 9 MPa
- 621 • at c. 250 m depth, the stress ratio is broadly 2:1.5:1. ( $\sigma_H:\sigma_h:\sigma_v$ ).

622 The current *in situ* stress regime is therefore aligned within the Triassic to earliest Jurassic thrusting  
623 regime that produced the Murai and Pasir Laba thrust faults and the broad range of brittle fault  
624 orientations interpreted in the bedrock geology of Singapore.

625

## 626 8. Conclusions

627 Middle to Upper Triassic, deep marine to fluvial volcano-sedimentary inner forearc strata  
628 assigned to Jurong and Sentosa group successions in Singapore (Dodd *et al.*, this volume) were  
629 deformed during compressional tectonics in the latest Triassic to earliest Jurassic climactic stages  
630 of Sundaland amalgamation and consolidation (*cf.* Hall, 2012; Metcalfe, 2017). Key features of  
631 the structural geology of Singapore include:

- 632 • Progressive shortening that transposed and tightened earlier-formed NW–SE trending  
633 inclined asymmetrical folds, culminating in the regional-scale development of a non-  
634 coaxial, NE-vergent and NE-facing, locally dextrally transpressive, fold and thrust system.
- 635 • The Murai Thrust and Pasir Laba Thrust are confirmed and extrapolated as major thrusts  
636 in this system; both structures are associated with SW-dipping imbricate thrust duplexes.
- 637 • The subduction-related magmatic complex represented by granitic to gabbroic plutons of  
638 the Bukit Timah Centre likely acted as a backstop to thrusting at this time.
- 639 • Lower Cretaceous Kusu and Bukit Batok formation strata overstep the orogenic  
640 deformation.
- 641 • Linked arrays of mostly NE–SW and ENE–WSW trending faults had developed by the late  
642 Cretaceous (possibly Cenomanian at least), and are an important control upon the surface  
643 and sub-surface distribution of bedrock units in Singapore.

- 644       • The disposition and movement history of these brittle faults was strongly influenced by  
645           dextral shear stress aligned parallel to Peninsular Malaysia, though this deformation will  
646           likely have reactivated faults initiated during Mesozoic orogenesis, or even earlier.

647  
648   An understanding of the distribution and geotechnical impact of these structural features will be  
649   important for both future development and ongoing management of the subsurface in Singapore.

650  
651   **Acknowledgements:** Many colleagues in the British Geological Survey and collaborators in  
652   Singapore, including KoKo Lat, Michael Goay, Lau Sze Ghiong, Lim Yong Siang, Kyaw Zin,  
653   Zaw Min Hlaing in BCA, have contributed to this study, given freely of their advice, and provided  
654   the local knowledge so important to understanding Singapore’s geology. BGS would like  
655   particularly to thank Kiso-Jiban Consultants Co. Ltd for their assistance and considerable  
656   contribution to the investigative works on the geology of Singapore. The authors also acknowledge  
657   Dr Grahame Oliver’s contributions to many thought-provoking and informative discussions  
658   concerning all aspects of Singapore geology. Dr Amy Gough and an anonymous referee are  
659   thanked for thoughtful and critical reviews that have greatly improved the manuscript. All  
660   diagrams and images included in this paper have been drafted and produced by Craig Woodward,  
661   BGS. The paper is published by permission of the executive directors of the British Geological  
662   Survey (UKRI) and the Building and Construction of Authority of Singapore (BCA).

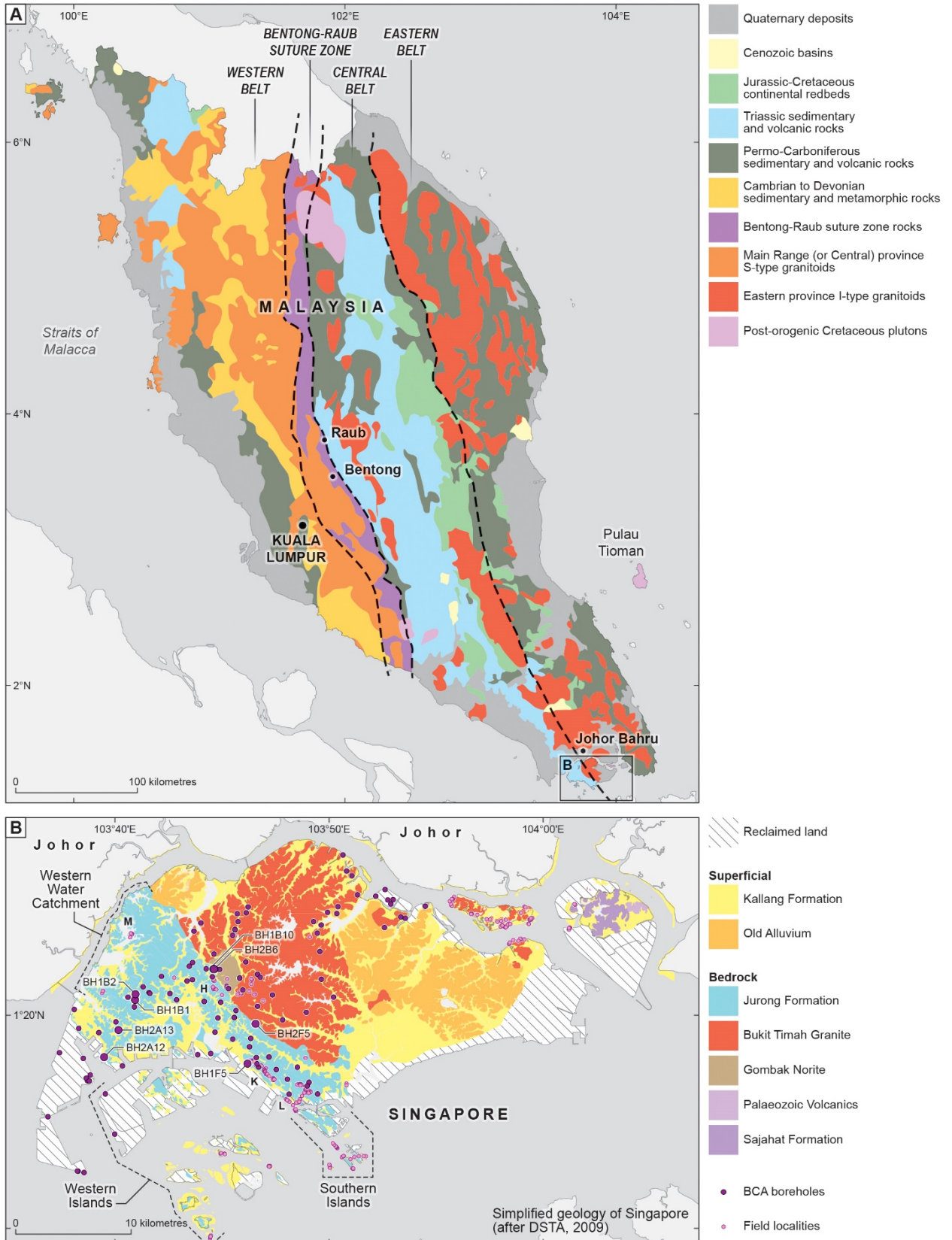
663

664 **References**

- 665 Abdullah, N. T., 2009. Mesozoic Stratigraphy. In: Geology of Peninsular Malaysia. Hutchison,  
666 C.S. and Tan, D. N. K. (eds.), (Kuala Lumpur: University of Malaya and Geological Society of  
667 Malaysia), pp 87-129.
- 668 Carter, A., Roques, D., Bristow, C. and Kinny, P., 2001. Understanding Mesozoic accretion in  
669 Southeast Asia: significance of Triassic thermotectonism (Indosinian orogeny) in Vietnam.  
670 *Geology*, 29, 211-214.
- 671 Dodd, T.J.H., Gillespie, M.R., Leslie, A.G., Kearsy, T.I., Kendall, R.S., Bide, T.P., Dobbs, M.R.,  
672 Millar, I.L., **Lee, M.K.W., Chiam, K.S.L., and Goay, M.** 2019. **Paleozoic to Cenozoic sedimentary**  
673 **bedrock geology and lithostratigraphy of Singapore.** <https://doi.org/10.1016/j.jseas.2019.103878>  
674 **This volume.**
- 675 DSTA, 2009. Geology of Singapore 2nd Edition. Defence Science and Technology Agency.
- 676 Fromaget, J., 1932. Sur la structure des Indosinides. *CR Hebd. Seances Acad. Sci.* 195, p.538.
- 677 Fromaget, J., 1941. L'Indochine française, sa structure géologique, ses roches, ses mines et leurs  
678 relations possibles avec la tectonique. *Bulletin du Service Géologique de l'Indochine*. 26, 1–140.
- 679 Gillespie, M.R., Kendall, R.S., Leslie, A.G., Millar, I.L., Dodd, T.J.H., Kearsy, T.I., Bide, T.P.,  
680 **Goodenough, K.M.,** Dobbs, M.R., **Lee, M.K.W.,** and Chiam, **K.S.L.,** 2019. The igneous rocks of  
681 Singapore: new insights to Palaeozoic and Mesozoic assembly of the Sukhothai Arc. **This volume.**
- 682 Hall, R., 2009. The Eurasian SE Asian margin as a modern example of an accretionary orogen.  
683 351-372 in *Earth Accretionary Systems in Space and Time*. Cawood, P. A. and Kroner, A. (eds.),  
684 Geological Society Special Publication, 318 (London: Geological Society of London).
- 685 Hall, R., 2012. Late Jurassic–Cenozoic reconstructions of the Indonesian region and the Indian  
686 Ocean. *Tectonophysics*, 570, 1-41.
- 687 Harbury, N. A., Jones, M. E., Audley-Charles, M. G., Metcalfe, I. and Mohamed, K. R., 1990.  
688 Structural evolution of Mesozoic Peninsular Malaysia. *Journal of the Geological Society*. 147, 11-  
689 26.
- 690 Hutchison C.S. and Tan D.N.K., 2009. Geology of Peninsular Malaysia. Hutchison, C.S. and Tan,  
691 D. N. K. (eds.), (Kuala Lumpur: University of Malaya and Geological Society of Malaysia), 479  
692 pp., ISBN: 978-983-44296-9.
- 693 Krabbendam, M. and Leslie, A.G., 2010. Lateral variations and linkages in thrust geometry: the  
694 Traligill transverse zone, Assynt Culmination, Moine thrust belt, NW Scotland. In: Law, R.D.,  
695 Butler, R.W.H., Holdsworth, R.E., Krabbendam, M. and Strachan, R.A. (eds) *Continental*  
696 *tectonics and Mountain Building: the Legacy of Peach and Horne*. Geological Society, London,  
697 Special Publications, 335, 335-357.
- 698 Liew, T. C. and McCulloch, M. T., 1985. Genesis of granitoid batholiths of Peninsular Malaysia  
699 and implications for models of crustal evolution: Evidence from a Nd-Sr isotopic and U-Pb zircon  
700 study. *Geochimica et Cosmochimica Acta*. 49, 587-600.
- 701 Leslie, A.G., Krabbendam, M., Kimbell, G.S. and Strachan, R.A., 2010. Regional-scale lateral  
702 variation and linkage in ductile thrust architecture: the Oykel Transverse Zone, and mullions, in  
703 the Moine Nappe, NW Scotland. In: Law, R.D., Butler, R.W.H., Holdsworth, R.E., Krabbendam,  
704 M. and Strachan, R.A. (eds) *Continental tectonics and Mountain Building: the Legacy of Peach*  
705 *and Horne*. Geological Society, London, Special Publications, 335, 359-381.

- 706 McClay, K.R., 2013. The mapping of geological structures. John Wiley & Sons.
- 707 Meng, W., Chen, Q. C., Du, J. J., Feng, C. J., Q, X. H., An, Q. M., 2012. In situ stress  
708 measurements in Singapore. *Chinese Journal of Geophysics*. 55, 429-437.
- 709 Metcalfe, I., 1990. Stratigraphic and tectonic implications of Triassic conodonts from northwest  
710 Peninsular Malaysia. *Geological Magazine*, 127, 567-578.
- 711 Metcalfe, I., 2011. Palaeozoic-Mesozoic history of SE Asia. in *The SE Asian Gateway: History  
712 and Tectonics of the Australia-Asia Collision*. Hall, R., Cottam, M. A. and Wilson, M. E. J.  
713 (editors). Geological Society of London Special Publication, 355, 7-35. (London: Geological  
714 Society of London).
- 715 Metcalfe, I., 2013. Tectonic Evolution of the Malay Peninsula. *Journal of Asian Earth Sciences*, 76,  
716 pp.195-213.
- 717 Metcalfe, I., 2017. Tectonic evolution of Sundaland. *Bulletin of the Geological Society of  
718 Malaysia*. 63, 27-60.
- 719 Mustaffa, K. S., 2009. Structures and Deformation. in *Geology of Peninsular Malaysia*. Hutchison,  
720 c.S. and Tan, D. N. K. (editors). (Kuala Lumpur: University of Malaya and Geological Society of  
721 Malaysia).
- 722 Ng, S. W. P., Whitehouse, M. J., Searle, M. P., Robb, L. J., Ghani, A. A., Chung, S. L., Oliver, G.  
723 J.H., Sone, M., Gardiner, N. J. and Roselee, M. H., 2015a. Petrogenesis of Malaysian granitoids  
724 in the Southeast Asian tin belt: Part 1. Geochemical and Sr-Nd isotopic characteristics. *Geological  
725 Society of America Bulletin*, 127, 1209-1237.
- 726 Ng, S. W. P., Whitehouse, M. J., Searle, M. P., Robb, L. J., Ghani, A. A., Chung, S. L., Oliver, G.  
727 J.H., Sone, M., Gardiner, N. J. and Roselee, M. H., 2015b. Petrogenesis of Malaysian granitoids  
728 in the Southeast Asian tin belt: Part 2. U-Pb zircon geochronology and tectonic model. *Geological  
729 Society of America Bulletin*, 127, 1238-1258.
- 730 Oliver, G. J. H., Zaw, K. and Hotson, M., 2011. Dating Rocks in Singapore. *Innovation Magazine*.  
731 10, 22-25.
- 732 Oliver, G. and Prave, A., 2013. Palaeogeography of Late Triassic red-beds in Singapore and the  
733 Indosinian Orogeny. *Journal of Asian Earth Sciences*, 76, 214-224.
- 734 Oliver, G. J. H., Zaw, K., Hotson, M., Meffre, S. and Manka, T., 2014. U–Pb zircon geochronology  
735 of Early Permian to Late Triassic rocks from Singapore and Johor: A plate tectonic  
736 reinterpretation. *Gondwana Research*, 26, 132-143.
- 737 Oliver G.J.H. and Gupta A., 2019. *A Field Guide to the Geology of Singapore*. 2nd Edition. Lee  
738 Kong Chian Natural History Museum, National University of Singapore, Singapore.
- 739 Ori, G. G. and Friend, P. F., 1984. Sedimentary basins formed and carried piggyback on active  
740 thrust sheets. *Geology*, 12, 475-478.
- 741 Redding, J. and Christensen, J. B., 1999. *Geotechnical Feasibility Study into Rock Cavern  
742 Construction in the Jurong Formation*. (Singapore: Nanyang Technological University).
- 743 Searle, M. P., Whitehouse, M. J., Robb, L. J., Ghani, A. A., Hutchison, C.S., Sone, M., Ng, S. P.,  
744 Roselee, M. H., Chung, S. L. and Oliver, G. J. H., 2012. Tectonic evolution of the Sibumasu–  
745 Indochina terrane collision zone in Thailand and Malaysia: constraints from new U–Pb zircon  
746 chronology of SE Asian tin granitoids. *Journal of the Geological Society*, 169, 489-500.

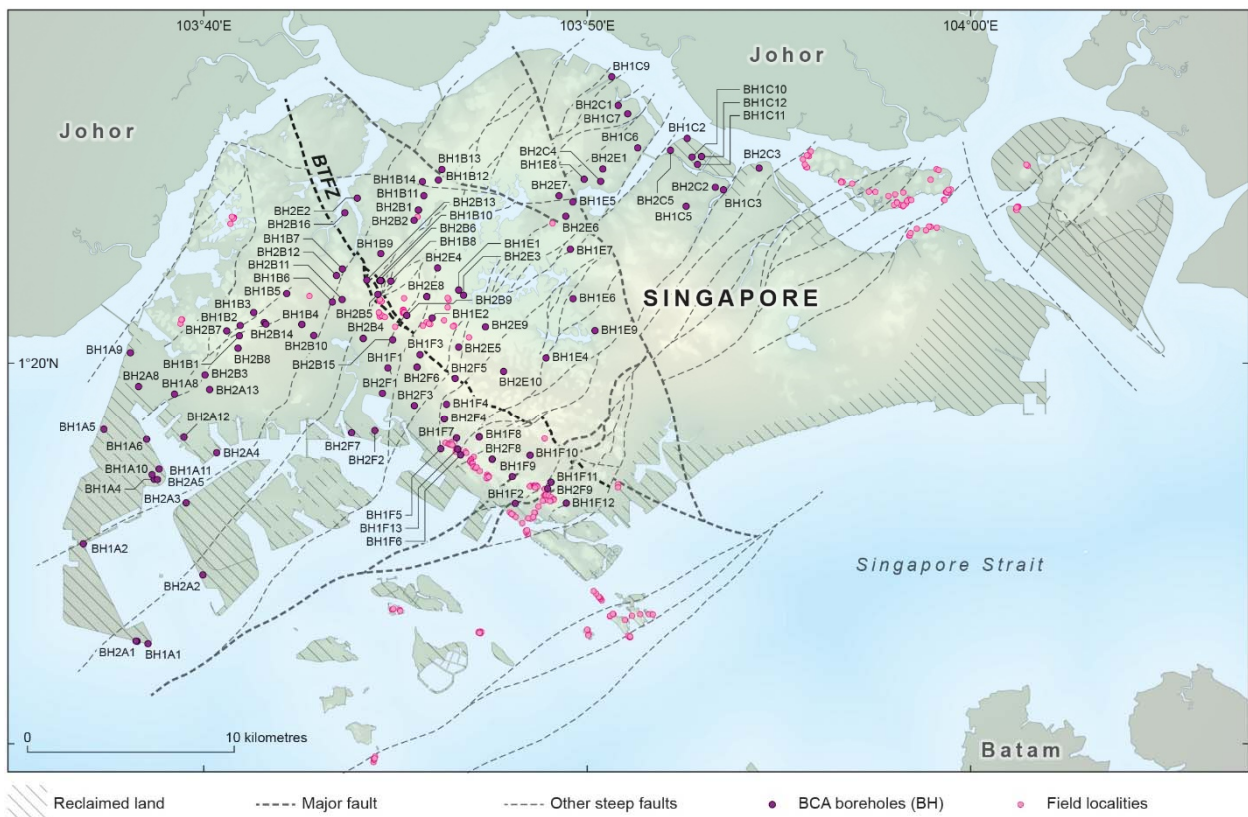
- 747 Sevastjanova, I., Clements, B., Hall, R., Belousova, E. A., Griffin, W. L. and Pearson, N., 2011.  
748 Granitic magmatism, basement ages, and provenance indicators in the Malay peninsula: Insights  
749 from detrital zircon U-Pb and Hf-isotope data. *Gondwana Research*, 19, 1024-1039.
- 750 Sone, M. and Metcalfe, I., 2008. Parallel Tethyan sutures in mainland Southeast Asia: New  
751 insights for Palaeo-Tethys closure and implications for the Indosinian orogeny. *Comptes Rendus*  
752 *Geoscience*, 340, 166-179.
- 753 Van Tri, Tran, Khuc, Vu (Eds.), 2011. *Geology and Earth Resources of Vietnam*, General Dept.  
754 of Geology, and Minerals of Vietnam, Hanoi, Publishing House for Science and Technology, p.  
755 634.
- 756 Vilpponen, A. M. B., 1988. *The Sedimentology and Stratigraphy of the Jurong Formation*,  
757 Singapore (Doctoral dissertation, National University of Singapore, unpublished).
- 758 Winn, K. and Ng, M., 2013. In situ stress measurements in Singapore. In: *Advances in*  
759 *Geotechnical Infrastructure*. Eds: Leung, C. F., Goh, S. H. and Shen, R. F. Singapore: Research  
760 Publishing.
- 761 Winn, K., Wong, L.N.Y., Zaw, K. and Thompson, J., 2018. The Ayer Chawan Facies, Jurong  
762 Formation, Singapore: Age and observation of syndepositional pyroclastic sedimentation process  
763 with possible peperite formation. *Bulletin of the Geological Society of Malaysia*, 66, 25-31.
- 764 Zhang, J., Sinclair, H.D., Li, Y., Wang, C., Persano, C., Qian, X., Han, Z., Yao, X. and Duan, Y.,  
765 2019. Subsidence and exhumation of the Mesozoic Qiangtang Basin: Implications for the growth  
766 of the Tibetan plateau. *Basin Research*, 1-28.
- 767 Zhao, J., Ashraf, M. H. and Zhou, Y., 2005. *Hydrofracturing in Situ Stress Measurements in*  
768 *Singapore Granite*. NTU Magazine - Civil Engineering Research. Singapore: Nanyang  
769 Technological University.



775 A – Simplified regional geological map of Peninsular Malaysia and Singapore including the  
 776 tectono-stratigraphical Western, Central and Eastern belts, and the trace of the Bentong–Raub  
 777 Suture Zone that marks the orogenic suture between Sibumasu (Western Belt) and the Sukhothai  
 778 Arc (Central and Eastern belts), (after Metcalfe, 2013). This suture zone apparently passes some  
 779 50–100 km west of Singapore. Boxed area is shown in more detail in map B of Singapore.

780 B – Simplified, previously published, geological map of Singapore (box in A), showing the  
 781 principal geological units (all unit names as previously published by DSTA, 2009). The  
 782 Mesozoic (meta)sedimentary ‘Jurong Formation’ strata of southern and southwest Singapore  
 783 shown here in blue should now be assigned to the Jurong and Sentosa groups (Dodd *et al.*, this  
 784 volume and Fig. 3). The location of new borehole cores acquired by BCA and described by BGS  
 785 are superimposed (see also Fig.2), as well as the outcrop locations examined by BGS across  
 786 Singapore; H – Hillside Park; K – Kent Ridge; L – Labrador Park; M – Murai Reservoir.  
 787 Boreholes specifically referred to in the text are labelled.

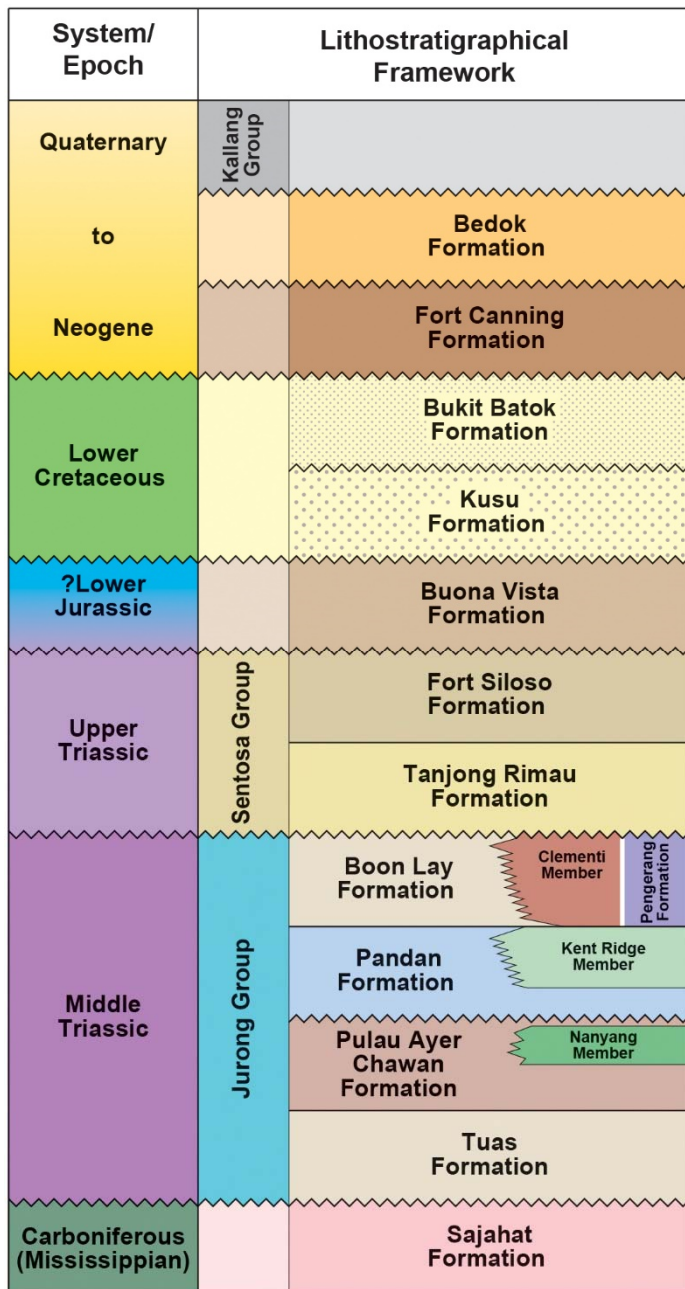
788



789

790 Figure 2

791 The distribution of BCA boreholes and field localities analysed as part of this study,  
 792 superimposed on a new, and here simplified, geological linework showing the major geological  
 793 boundaries including thrusts and other faults (*cf.* Figure 4). The Bukit Timah Fault Zone (BTFZ)  
 794 essentially forms a boundary between the pre-Cenozoic (meta)sedimentary and igneous rocks of  
 795 Singapore. In general, this study focuses on the boreholes and field localities in metasedimentary  
 796 rocks in the southern and western parts of Singapore (see also Dodd *et al.*, this volume); the  
 797 remainder mainly access the igneous rocks of the Bukit Timah Centre (Gillespie *et al.*, this  
 798 volume).

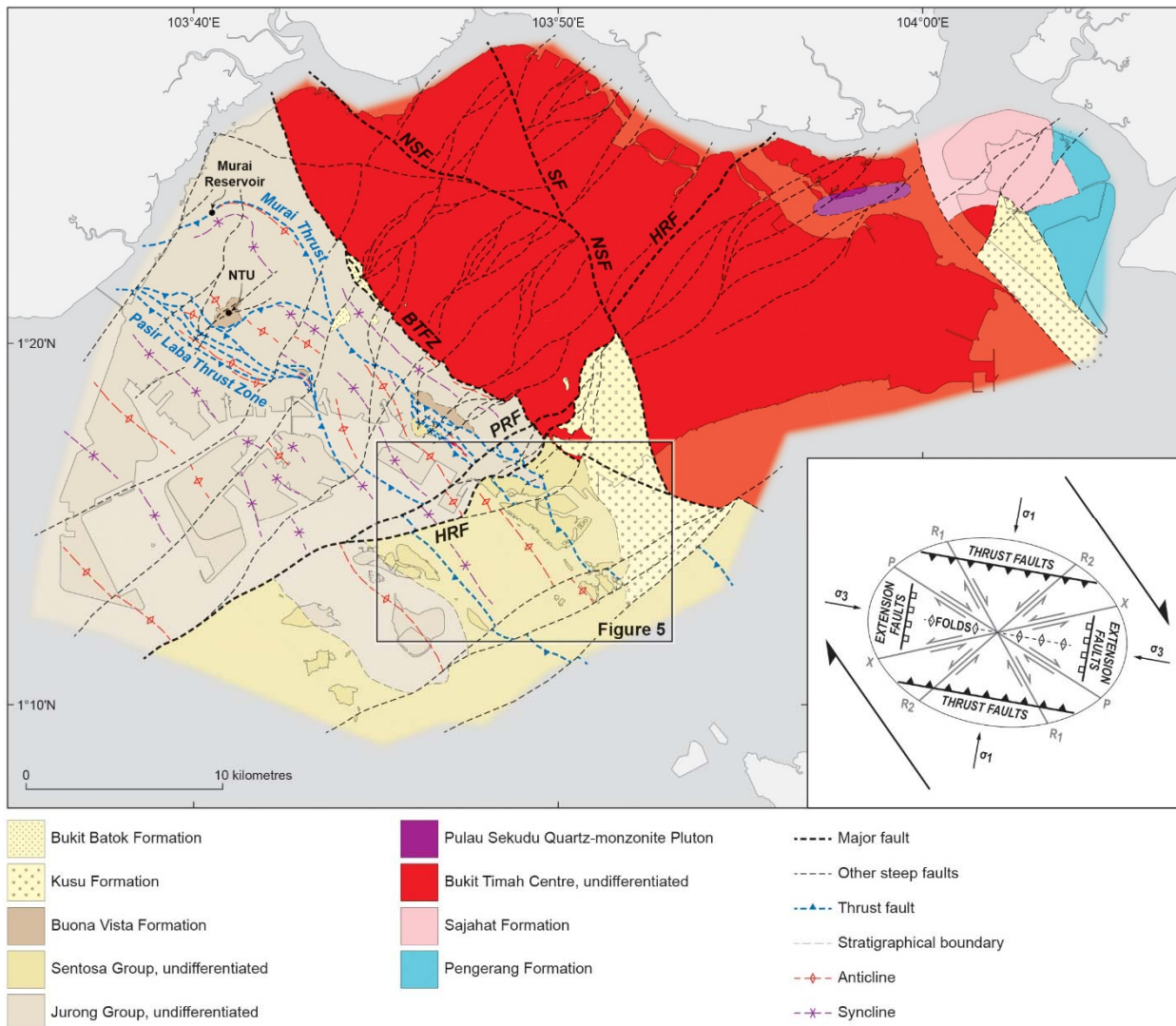


823

824 Figure 3

825 ICS-compliant lithostratigraphical column for Singapore bedrock geology. The Jurong Group is  
 826 now subdivided as four new formations, the Sentosa Group comprises two new formations. The  
 827 strata comprising these two groups in Singapore were formerly referred to collectively as the  
 828 Jurong Formation (DSTA, 2009). The Lower Cretaceous Kusu and Bukit Batok formations have  
 829 not previously been identified and were also previously assigned as Jurong Formation strata. The  
 830 Fort Canning Formation and Bedok Formation are ICS-compliant names for the Fort Canning  
 831 Boulder Bed and Old Alluvium respectively (*cf.* DSTA, 2009). This new lithostratigraphical  
 832 framework for Singapore is formalised in Dodd *et al.* (this volume).

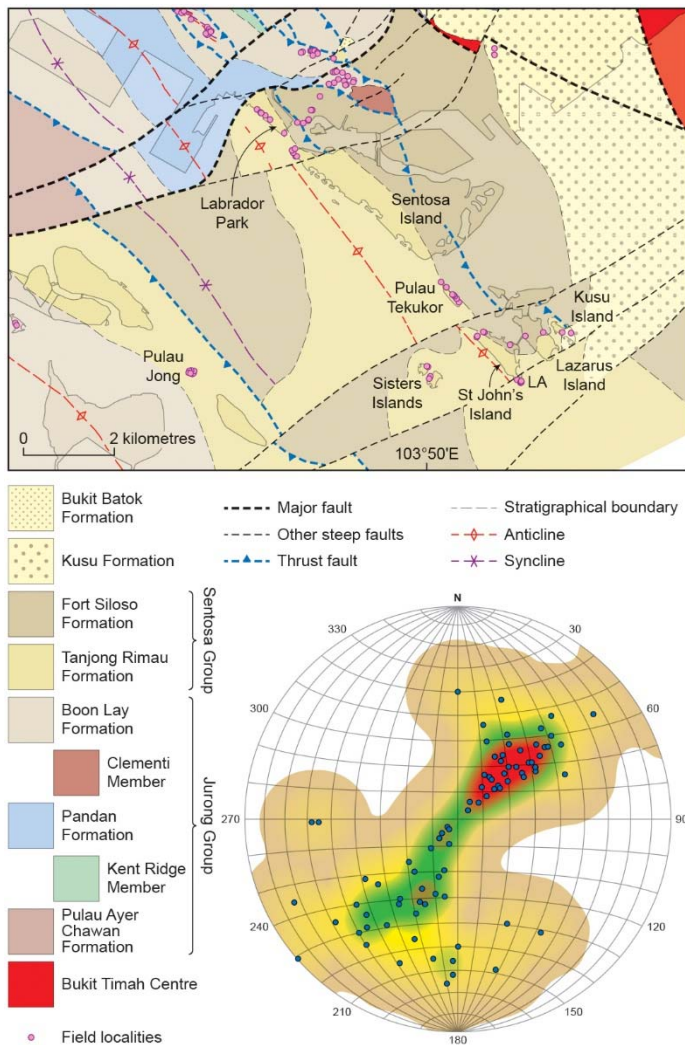
833



834

835 Figure 4

836 Revised but simplified geological map of Singapore derived from our interpretation of all  
 837 available BCA data, including offshore bathymetrical data that provides some measure of  
 838 constraint on fault patterns offshore. The map shows the principal geological units with the  
 839 major fold, thrust, and fault structures superimposed. The Mesozoic Jurong and Sentosa group  
 840 outcrops are shown undivided for clarity (*cf.* Figure 3). ‘Murai Reservoir’ is highlighted as a key  
 841 exposure of the Murai Thrust in western Singapore; NTU – Nanyang Technological University  
 842 campus (see text). Named brittle faults are labelled: HRF - Henderson Road Fault; PRF - Pepys  
 843 Road Fault; NSF - Nee Soon Fault; SF – Seletar Fault; BTFZ - Bukit Timah Fault Zone. Boxed  
 844 area is shown in more detail in Figure 5. The inset strain ellipse shows the array of fault  
 845 orientations in Singapore in relation to a predicted maximum compressive stress direction,  $\sigma_1$   
 846 (redrawn after McClay, 2013).



867

868 Figure 5

869 Bedrock geological map of southern Singapore, including the 'Southern Islands'; key field  
 870 localities visited are superimposed on the formation level lithostratigraphy (*cf.* Fig. 3). LA –  
 871 Lokos Anticline at Tanjong Lokos, St. John's Island. The stereonet shows bedding  
 872 measurements in Sentosa Group strata from Sentosa Island and Labrador Park to St. John's and  
 873 Lazarus Islands (equal area lower hemisphere projection,  $n = 81$ ), NW–SE trending folding is  
 874 clearly demonstrated.

875



876  
 877 Figure 6  
 878 A – Hinge area of a metre-scale anticline in sandstone and mudstone, northern shore of Pulau  
 879 Jong. View to south-east, the hammer shaft is 35 cm long. (Locn. AGLE\_156, [22769.9  
 880 22039.0]).  
 881 B – Well-developed discrete planar S1 foliation, in steeply NE-dipping planar laminated fine  
 882 sandstone and mudstone, northern shore of St. John's Island, Fort Siloso Formation. Profile view  
 883 looking to the south-east. (Locn. KMGO\_5, [29827.8 22611.9]).

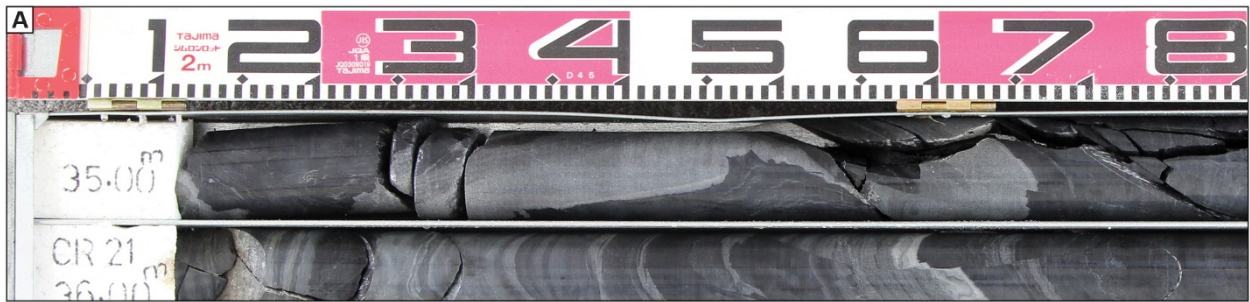
884 C – Lazarus Island: Interbedded sandstone and siltstone, Fort Siloso Formation. S0 dips NE, and  
885 S1 is clearly seen in all lithologies (aligned parallel with compass-clinometer), and is clearly  
886 refracted across mudstone/sandstone layers. View to south-east. (Locn. KMGO\_6, [30169.0  
887 22806.0]).

888 D – Lokos Anticline in Tanjong Rimau Formation strata, St. John's Island (Fig. 4). The fold is  
889 asymmetrical with a more steeply-dipping, and more intensely cleaved and rotated north-eastern  
890 limb to the right of the anticlinal hinge in this view. The S1 cleavage on the southwest limb dips  
891 steeply to the south-west and is north-east verging; an intense SW-dipping fracture cleavage  
892 occurs on the progressively rotated north-eastern limb of the fold. View to north-west,  
893 foreground figure is 1.8 m tall. (Locn. AGLe\_140, [30070.8 21786.9]).

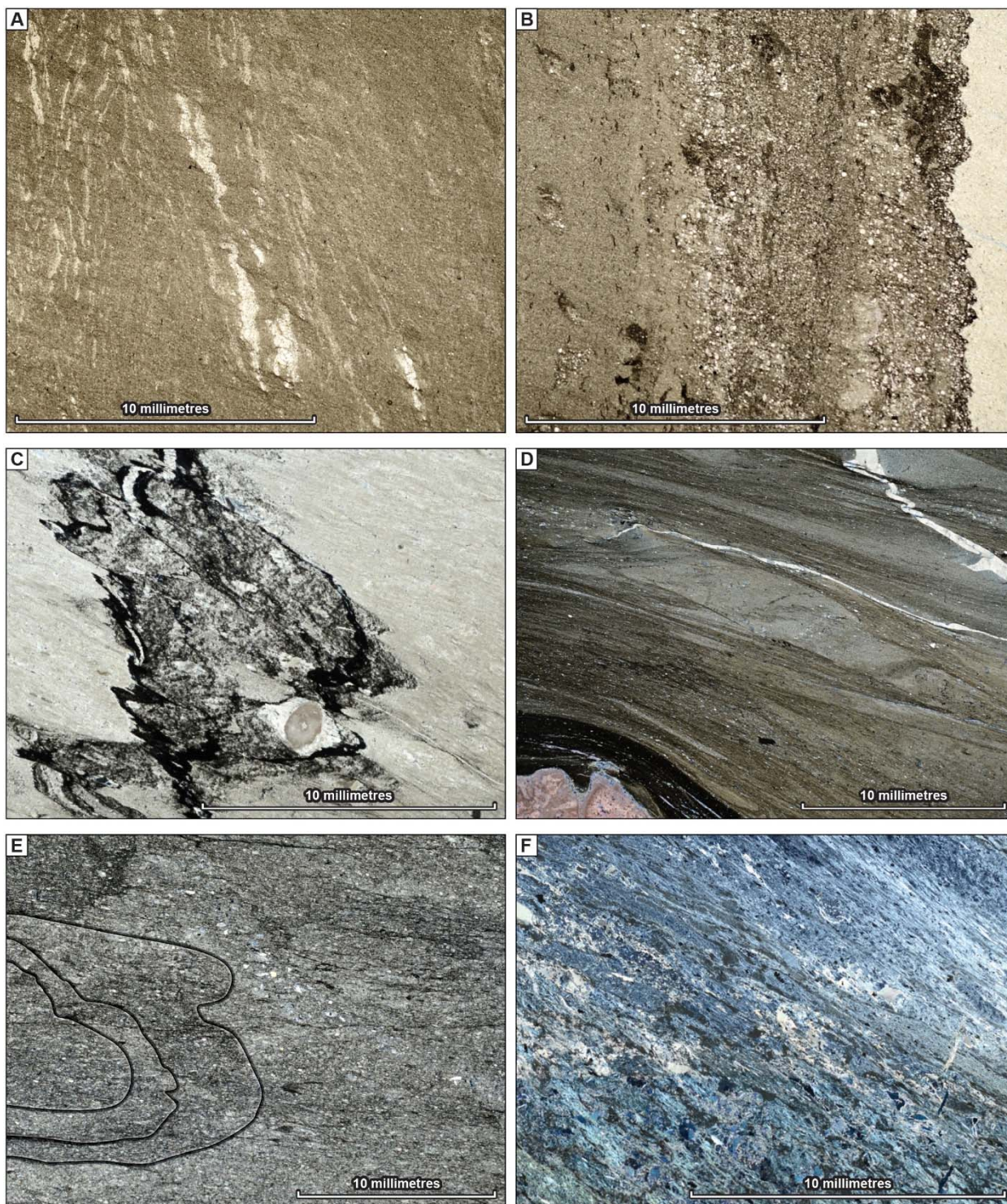
894 E – Intense south-west-dipping fracture cleavage, Lokos Anticline, St. John's Island. This  
895 feature occurs on the progressively transposed and steepened north-eastern limb of the fold.  
896 Tanjong Rimau Formation sandstone. The hammer shaft is 35 cm long. (Locn. AGLe\_140,  
897 [30070.8 21786.9]).

898 F – Intense, top-to-NE crushing/shearing in inner arc of Lokos Anticline, St. John's Island.  
899 Gently north-east-dipping coarse-gravel fluvial sandstone, Tanjong Rimau Formation. View to  
900 north-west, hammer head is 15 cm long. (Locn. AGLe\_140, [30070.8 21786.9]).

901



902  
 903 Figure 7  
 904 A – Fold closure in Pulau Ayer Chawan Formation sandstone and mudstone, BH2A12 [31439.2  
 905 08515.2]. The sharp basal boundary of the pale grey sandstone against darker grey mudstone is  
 906 clearly folded across the core, locally becoming inverted. The scale bar is marked off in 10 cm  
 907 intervals.  
 908 B – Core surface showing well-developed anastomosing S1 fabric, BH2A12. Note associated  
 909 micro-offsets of the light grey sandstone/dark grey mudstone boundary indicating non-coaxial  
 910 deformation.  
 911



912

913 Figure 8

914 Photomicrographs illustrating the development of the S1 fabric in Jurong Group strata.

915 A – BH1A11, 156.9–157.0 m. Siltstone, Pulau Ayer Chawan Formation. Penetrative S1 fabric  
 916 inclined left to right; dark iron-rich mineralisation on anastomosing pressure solution seams  
 917 accentuate this fabric. S1 arranged at a high angle to the steep bedding lamination (S0) in this  
 918 view. Note that micro-folding of S0 laminations is aligned on S1 as axial planer fabric. Plane-  
 919 polarised light (PPL) image.

920 B – BH1A11, 117.5–117.86 m. Recrystallized, locally bioclastic, mudstone and siltstone, Pulau  
 921 Ayer Chawan Formation, with conspicuous, pale coloured, fine-grained lithic-crystal-tuff

- 922 horizon (to right) Well-developed, penetrative, pressure solution S1 fabric at a high angle to S0  
923 laminations; non-coaxial simple shear fabric. Note micro-folding of S0 lamination at  
924 tuff/sandstone boundary. PPL image.
- 925 C – BH2A4, 127.8 - 128.0 m. Metalimestone. Pandan Formation. Intensely developed,  
926 anastomosing, S1 pressure solution fabric; axial planar close to tight folds of S0 lamination and  
927 black stylolitic seams (and of secondary calcite veins within those stylolite features). PPL image.
- 928 D – BH1A6, 161.2–161.40 m. Metamudstone, Pandan Formation. Very well-developed,  
929 intensely penetrative S1 anastomosing pressure solution fabric, with very tight folds of S0  
930 lamination arranged around axial planar S1 fabric. Note cross-cutting (pressure solution) calcite  
931 vein is folded in that same S1 fabric. Note also that fabric deflects around little-modified  
932 macrofossil fragments. Chlorite grows on this S1 fabric confirming epizone-grade  
933 metamorphism. PPL image.
- 934 E – BH1A8, 172.05–172.15 m. Metacarbonate rock, Pandan Formation. Well-developed S1  
935 fabric with axial planar relationship to close folds of S0 lamination (outlined). Pronounced grain-  
936 shape fabric in clastic quartz grains is aligned with S1. PPL image.
- 937 F – BH2A13, 160.15–160.35 m. Pyroclastic rock – ignimbrite, Pulau Ayer Chawan Formation.  
938 Strongly-developed S1 fabric (in sericite-chlorite trails), especially in upper left portion of view.  
939 Note that S1 is in an 'S/C' relationship with deformed fiamme and the earlier eutaxitic fabric in  
940 the ignimbritic groundmass (latter dominant in lower right of view). Cross-polarised image  
941 (XPL) image.
- 942

943 Figure 9  
 944 Murai Thrust: Western  
 945 Water Catchment, SAFTI  
 946 Live Firing Area. View  
 947 centred on Locn.  
 948 AGLe\_22, [10906.3  
 949 42099.4]. The line  
 950 interpretation (lower  
 951 panel) of the panorama  
 952 captured in the top panel  
 953 shows the antiformal  
 954 stacking of thrust  
 955 imbricates in Jurong  
 956 Group strata (Boon Lay  
 957 Formation), and  
 958 steepening of the trailing-  
 959 edge imbricate stack,  
 960 during top-to-NE tectonic  
 961 transport (to the left in this  
 962 image). View is to the  
 963 south-east; the outcrop is  
 964 some 18 to 20 m high.  
 965

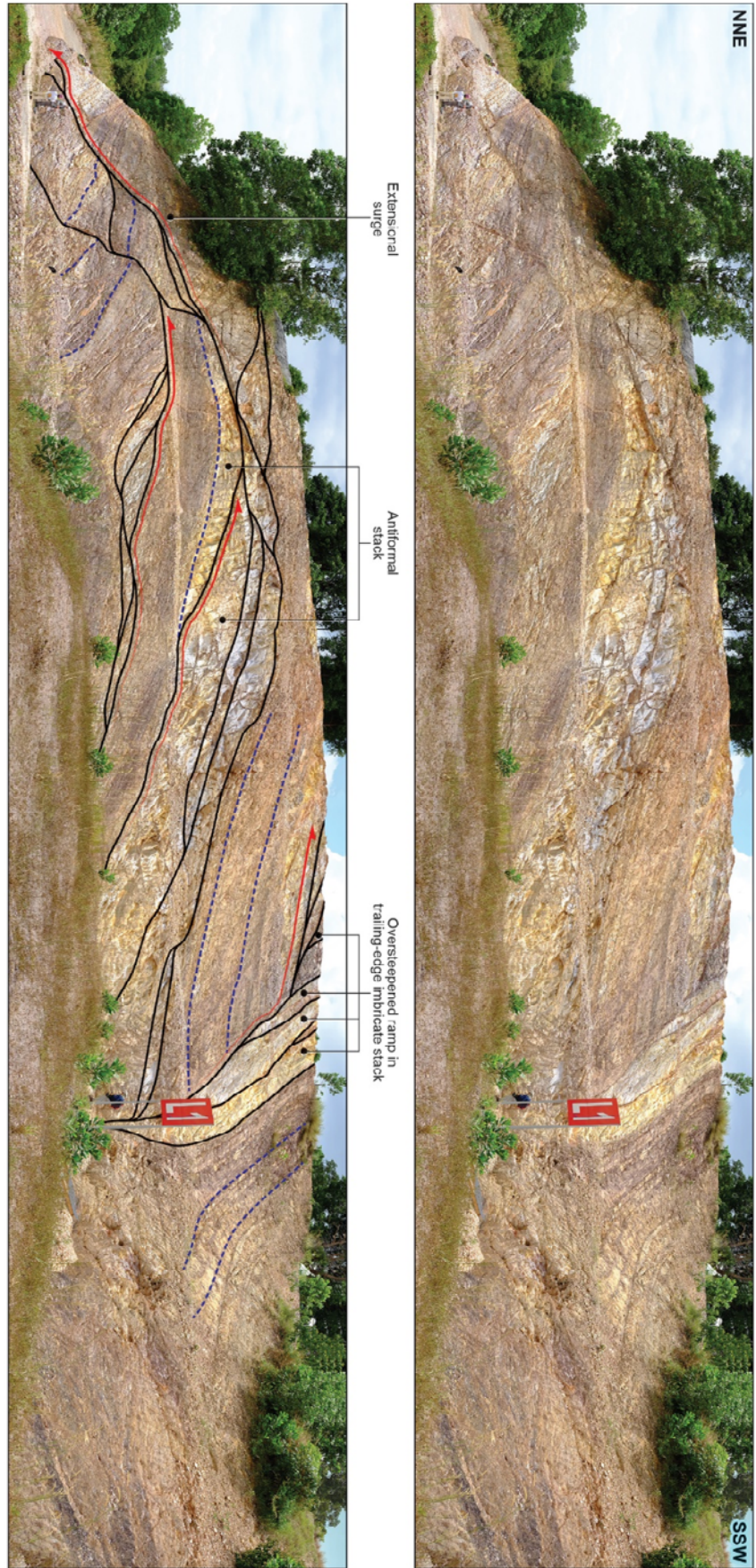
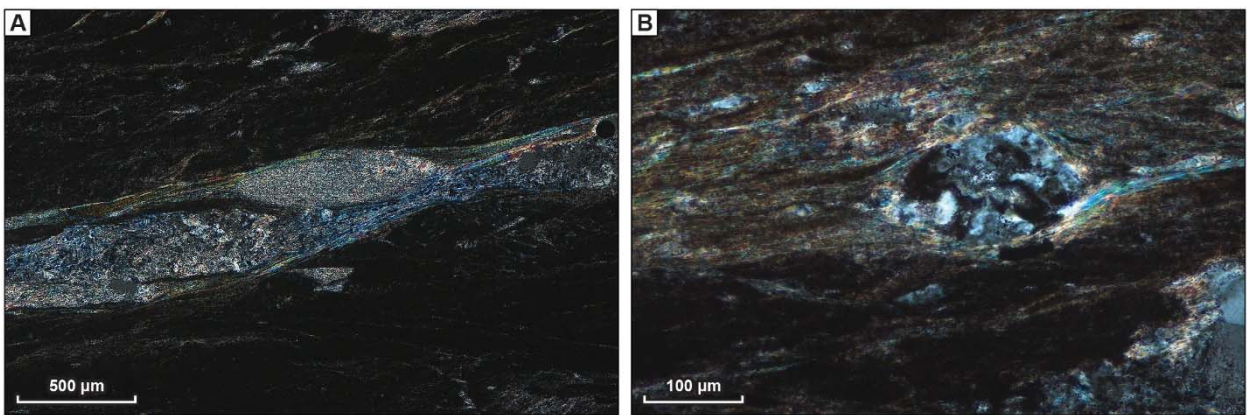




Figure 10

Murai Thrust: Locn. AGLe\_22, [10906.3 42099.4]). Secondary shears (highlighted) cross-cutting and modifying anastomosing shear fabric in Jurong Group strata to produce top-to-NE antiformal stacking. View to south-east, the hammer shaft is 35 cm long.

977



978

979 Figure 11

980 Murai Thrust: Locn. AGLe\_22, [10906.3 42099.4]. Shear indicators in phyllonitic mudstone,  
 981 Boon Lay Formation. A: elongate and stacked sericite 'mica fish' extending up to ~1.5 mm. B:  
 982 sigma porphyroblast formed from recrystallised, 'cherty' quartz in phyllonitic argillised matrix.  
 983 Quartz is only significantly recrystallized in these strata at these highest strains, indicating  
 984 lowermost epizone metamorphic conditions. In both cases the sense of shear is sinistral as shown  
 985 and top-to-the-NE in reality. XPL in both views.

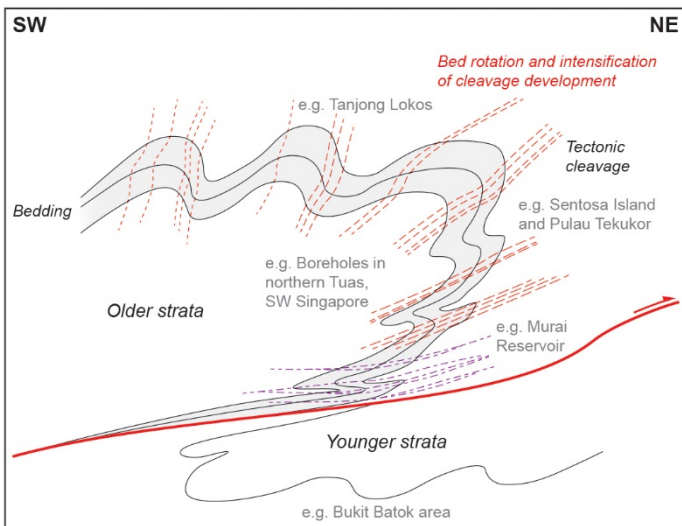
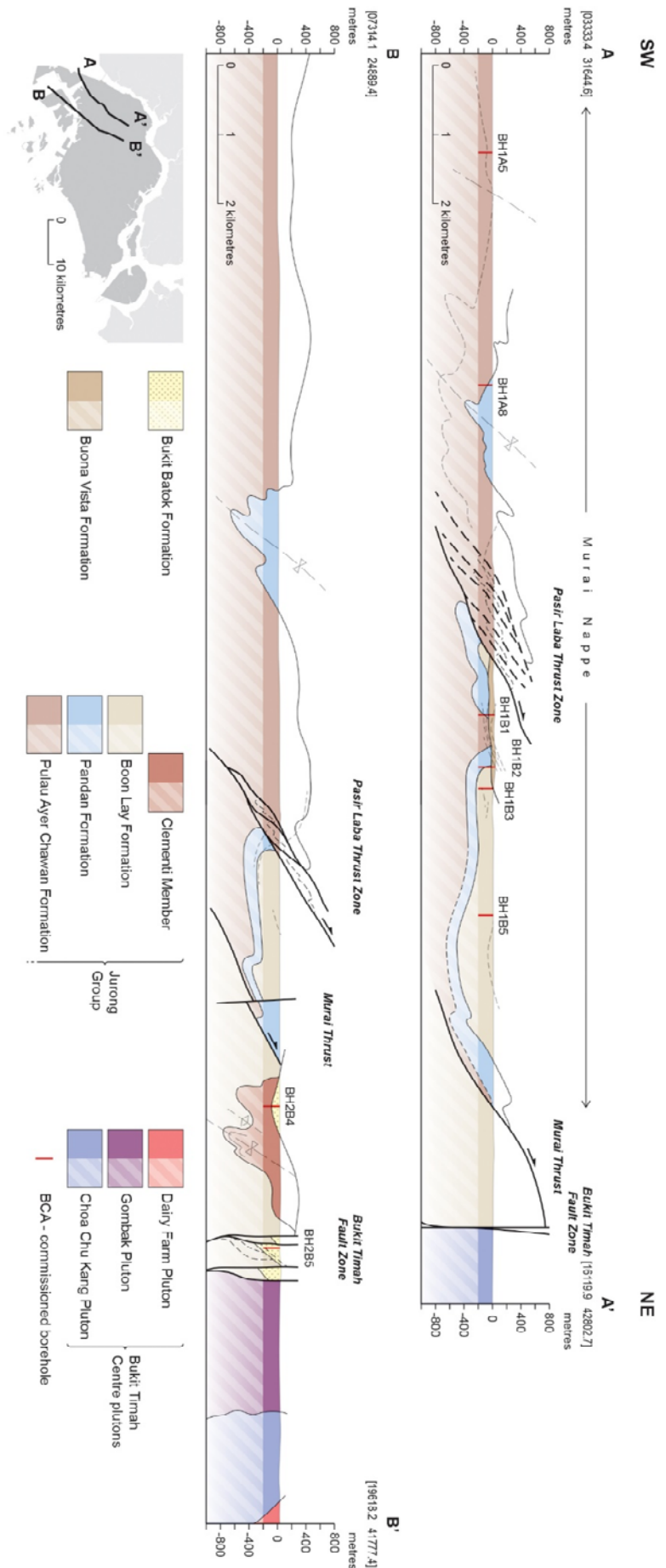


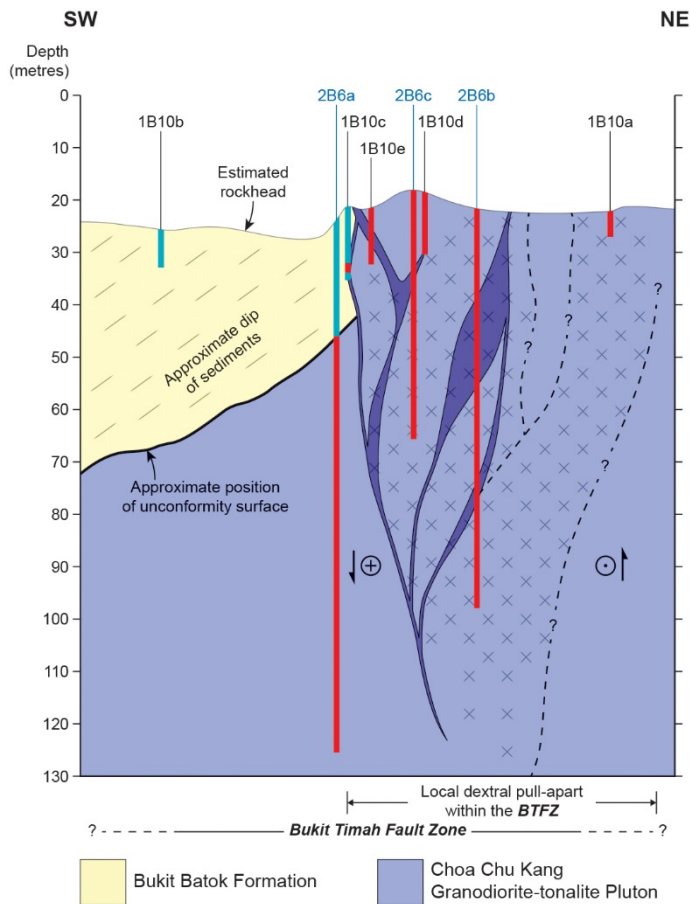
Figure 12

Composite cross-sectional schematic model for the ductile deformation of the Jurong and Sentosa group strata in southern and south-west Singapore. No specific structures are named in the model, see further discussion in text. The model is intended to be essentially scale-independent representing process.

997 Figure 13

998 Cross-sections constructed along  
 999 the lines A–A’ and B–B’ in south-  
 1000 west Singapore – see inset map  
 1001 lower left. These sections are  
 1002 representative of the digital 3D  
 1003 National Geological Bedrock  
 1004 Model of Singapore created by  
 1005 BGS for BCA and are based upon  
 1006 the overall understanding of the  
 1007 structural architecture of the  
 1008 sedimentary rocks examined in  
 1009 boreholes and outcrop across  
 1010 south-west Singapore. Steep faults  
 1011 are omitted for clarity. The solid  
 1012 colour bar in these images, and the  
 1013 superimposed linework, reflects  
 1014 the volume occupied by the  
 1015 individual formations and their  
 1016 boundaries and structure in the new  
 1017 digital bedrock model. The  
 1018 diagonal shading and linework  
 1019 below represents the likely  
 1020 extension of the model units at  
 1021 depth; likewise, the model  
 1022 linework is projected above the  
 1023 present ground surface. The  
 1024 lithostratigraphy in this part  
 1025 Singapore is represented at  
 1026 formation level and thus provides a  
 1027 greater degree of resolution than in  
 1028 the Figure 4 map.





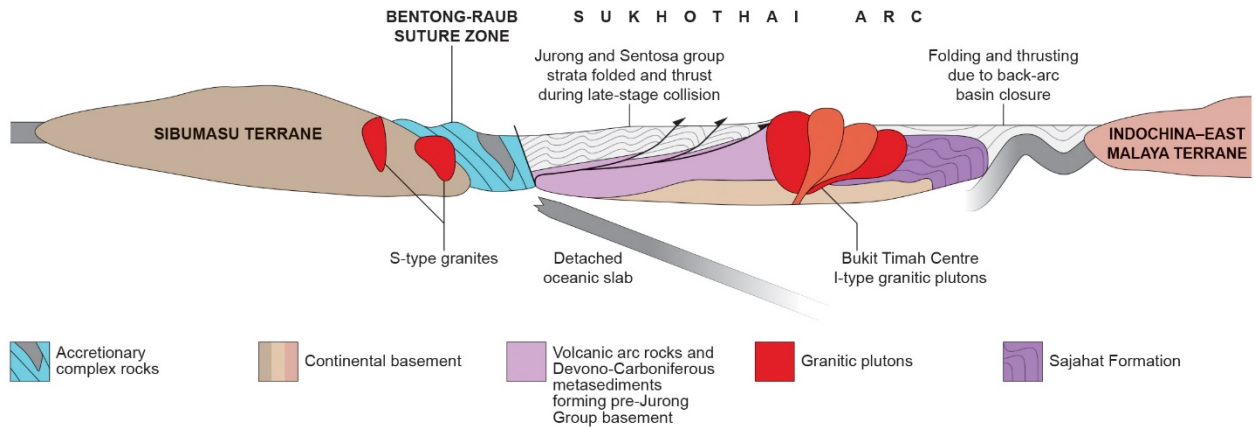
1044

1045 Figure 14

1046 Interpretation of the geology of the Bukit Timah Fault Zone from profiles of the BH1B10 and  
 1047 BH2B6 series boreholes (Figs. 1B and 2). Vertical and horizontal scales are identical. Vertical  
 1048 bars below rockhead represent cores; blue fill denotes sedimentary rocks in core, red fill denotes  
 1049 igneous rocks in core. Borehole identifiers are abbreviated (e.g., '1B10b' is an abbreviation of  
 1050 BH1B10b). 'X's denote areas where intervals or occurrences of fault-rock are observed and/or  
 1051 inferred. Dark blue = inferred position of fault strands. Half-arrows indicate the sense of the  
 1052 vertical component of displacement; '+' and '•' the horizontal component. See text for details of  
 1053 geological interpretation.

1054

Collision and amalgamation (late Triassic to early Jurassic, c. 200 Ma)



1055

1056 Figure 15

1057 Cartoon showing the tectonic evolution of the Singapore crustal region during late Triassic to  
 1058 earliest Jurassic times, and as it relates to the orogenic deformation in this now southern sector of  
 1059 Sibumasu and the Sukhothai Arc, and the amalgamation of Sundaland (after Sone and Metcalfe,  
 1060 2008; Ng *et al.* 2015a, b; Metcalfe, 2017; Dodd *et al.*, this volume; Gillespie *et al.*, this volume).  
 1061 The Sibumasu and Indochina-East Malaya terranes are shown in highly simplified form but see  
 1062 also Metcalfe (2017) for details of these elements.